Measuring the Impacts of Climatic Exposure to Pavement Surface Deterioration with Low Cost Technology

Zakariya, Gadi

A Thesis
In
the Department
Of
Building, Civil and Environmental Engineering

Presented in Partial Fulfillment of the Requirements
for the Degree of Master of Applied Science at
Concordia University
Montreal, Quebec, Canada

March, 2018

CONCORDIA UNIVERSITY

Schools of Graduate Studies

This is to certify that the thesis prepared

By: Zakariya, Gadi

Entitled: Measuring the Impacts of Climatic Exposure to Pavement Deterioration with Low Cost Technology

and submitted in partial fulfillment of the requirements for the degree of

Master of Applied Science

Complies with the regulations of the University and meets the accepted standards with respect to originality and quality.

Signed by the final examining committee:

_____ TBA - Chair

_____ Dr. Ciprian Alecsandru – Examiner

_____ Dr. Ali Nazemi - Examiner

_____ Dr. Amin Hammad - External Examiner

_____ Dr. Luis Amador Jimenez - Supervisor

Approved by

_____

Chair of Department or Graduate Program Director

_____

Dean of Faculty

Date _____

ABSTRACT

Measuring the Impacts of Climatic Exposure
to Pavement Surface Deterioration
with Low Cost Technology

Zakariya, Gadi

Pavements play a significant role in social and economic development. Canada spent approximately 12 billion dollars annually on pavements. However, roads are exposed to climatic changes and truck loads which affect their serviceability and reduce their lifespan. Most of Canada is exposed to freeze-thaw cycles which have a drastically impact on the pavement structure. A large portion of the deterioration occurs during the spring thaw period.

This research uses a smartphone to estimate pavement roughness on a weekly basis during 30 weeks in an attempt to test if such indicator can be used to identify the beginning of the load restriction and the overall damage experienced after one environmental cycle. A pavement section located on highway 20 near Montreal was visited during 2016 and 2017 season. The studied segment is about 8 km long. A pavement roughness index (RI) was estimated before, during, and after the winter season. The air temperature was registered in order to characterize the number of freeze thaw cycles experienced. It was impossible to use the RI measurements to identify the beginning of the thawing period as RI reflected the wheel-path driven and in many occasions changed were imperceptible. It was only after taking dates with larger time separation that overall decay in roughness condition was observed.

One day during Fall, Winter, and Spring selected as an excellent case to present the freeze-thaw cycle effect and to show the variations in the pavement surface condition. It has been found that the freeze-thaw cycle impacted the subgrade soil layer which reflected on the pavement surface. The average RI value before the frost season was found to be 3.99 m/km in average, while during winter season was 4.52 m/km, and in spring season was 5.30

m/km on average. The pavement deterioration was increased by average of 1.31 m/km. The results of RI change were then transferred into other Canadian location with dissimilar freezing index and annual precipitation, and annual impact of expected roughness decay estimated for various cities.

KEY WORDS:

Freeze-thaw; Frost heave period; pavement condition; International Roughness Index; Seasonal load restrictions; Excel; ArcGIS

DEDICATION

This work is dedicated to

mother, father, wife, daughter, brother, Sisters for their support through the years

ACKNOWLEDGEMENTS

I am here to show my sincere gratitude to my supervisor *Dr. Luis Amador* for his ardent advice, guidance, encouragement and good relationship during this research work. I would like to thank him also for encouraging me to increase my knowledge. Finally, I would like to thank him for his patience and cooperation during the thesis writing and correction period. The next thing, I would like to thank my family, my parents (*Fatma & Ahmed*), they always supported and encouraged me with their best wishes, my wife *Weam*, darling daughter *Mariam*, for pulling me up and believing in me to the end, my brother Yahya, my sisters, Rouida & Omima for their support. Lastly, I am very grateful to the *University of Tripoli (UOT)* for nominated me to receive a scholarship from the *Ministry of Higher Education and Scientific Research (MHESR)*, Libya.

TABLE OF CONTENTS

LIST OF TABLES

LIST OF FIGURES

LIST OF ACHRONYMS

RI	Pavement Roughness Index
AASHTO	American Association of State Highway and Transportation Officials
DBP	Deflection Basin Parameters
FHWA	Federal Highway Administration
SLR	Seasonal Load Restriction
FPD	Frost Penetration Depth
WSDOT	Washington Department of Transportation
TI	Thawing Index
FI	Freezing Index
FWD	Falling Weight Deflectometer
DBP	Deflection Basin Parameter
SCI	Surface Curvature Index
BDI	Basin Damage Index
BCI	Basin Curvature Index
PSI	Present Serviceability Index
PCI	Pavement Condition Index
PQI	Pavement Quality Index
PRI	Pavement Rating Index
PDI	Pavement Distress Index
RPUG	Road Profiler User Group
HPMS	Highway Performance Monitoring System
RMS	Root Mean Square
ADT	Average Daily Traffic
GPS	Global Positioning System
ArcGIS	Geographic Information System
VIMS	Vehicle Intelligent Monitoring System
CSV	Comma Separated Vector

CHAPTER 1

1 Introduction

1.1 Background

Road pavements are exposed to different climatic conditions, in cold regions they are exposed to freeze thaw damage which accounts to substantial damage similar to that experience in tropical countries with expansive soils. Countries such as Canada, Norway, Sweden, Russia, Finland and etc., suffer various freeze-thaw cycles where the pavement subgrade soil freezes and heaves. An upward movement occurs in the subgrade layer resulting from the expansion of accumulated soil moisture as it freezes. After heaving the subgrade layer loses its stiffness resulting from soil saturation as ice within the soil melts. Moisture content increases the tensile strain and fatigue cracks sensitivity. Also, reduces resilience modulus of the subgrade layer under traffic loads. Indeed, pavement roughness deteriorates which cause an infliction and reduction in road service life as well as providing a poor quality of ride for commuters.

1.2 Problem Statement

Canada is a second largest country in the world with thousands of kilometers of road pavements. Millions of commuters and cargos move every day throughout the country which drastically impacts on the society and the economy of the country.

Weather variation and air temperature discrepancies in Canada play a significant role in pavement roughness distress. Every year Canada exposes to a freeze-thaw cycle which

creates a reduction in commuter's safety and consumes economic resources in repairs. Pavement roughness quality decreases throughout winter resulting from ice lenses and get worst in spring as the ice melts down. Pavement distress reflects on the pavement surface as distortions and fatigue cracks. Additionally, Canada spends approximately 12 billion dollar annually on pavement construction and maintenance. Protecting pavement surface from deterioration is a very challenging task. Hence the measurement of changes in pavement condition and prediction of the impact of freeze thaw cycles is a key to enforce truck load reductions and implement other operational measures to reduce pavement damage.

1.3 Research Objective

1.3.1 Overall Goal

The overall goal of this research is to measure the impacts of freeze-thaw cycles on pavement deterioration with low cost technology on site. First to test if RI progression can be used to identify the beginning and the end of the spring load reduction by matching such season with the period of time where larger RI deformations are observed. Secondly to test if mobile technology can capture the overall RI deterioration suffered after one environmental cycle.

1.3.2 Research Tasks

The following two tasks are required to address the general objective:

Task 1: This task characterizes the International Roughness Index (RI) and suggests the possibility to collect a proxy for RI with low cost instruments; utilizing cellphone mobile technology.

Task 2: This task estimates the RI differential after one year (and various freeze-thaw cycles) for a segment of highway in the vicinity of Montreal. The estimated variation of roughness is then used to estimate pavement deterioration in other locations with the aid of AASHTO's Mechanistic Empirical Pavement Design Guide.

1.4 Scope and Limitations

This research employs a low cost method to collect pavement surface condition data through out one environmental cycle and evaluates the pavement condition for the purpose of roughness comparison for different seasons. This research includes some limitations: the wheel path of each passage differs from the one before, however the averaging of many observations remove the bias introduce by this physical constraint. The data collected between September 2016 and May 2017 is specific for the environment cycle observed and its deviations from normal behavior when considering annual normal. Some factors in the equation used to finalize the RI values were limited and assumed through expert criteria. Hence these factors should be further studied on future studies.

1.5 Organization of the Thesis

This thesis is organized in five chapters as follows: chapter 1 includes a background of the freeze-thaw effect on pavement as well as explains the objectives and methods used. Chapter 2 contains the literature review, which contains thesis problem from different perspectives, the effect of the freeze-thaw cycle, the methods to assign the pavement roughness, pavement roughness indices, and a brief demonstration of the RI. Chapter 3 presents road profile section and location. Also, describes method and software used to record pavement roughness data. The method used divided into two stages: site work stage and computer work stage. Chapter 4 includes pavement surface roughness charts that show

the RI for different season as a purpose of comparison between each season. Additionally, the chapter shows the RI values utilized by an equation issued by AASHTO to compare pavement roughness in different cities in Canada. Finally, chapter 5 concludes the thesis and provides certain recommendations for future research.

CHAPTER 2

2 Literature Review

2.1 Introduction

This chapter reviews the main concepts related to pavement deterioration, especially from environmental cycles; it provides the technical background for the effect of freeze-thaw cycles and the weight restrictions practices. Methods for determining the load restriction are briefly explained. Finally, the last two sections are devoted to explain pavement condition, its assessment and the technicalities behind the estimation of pavement roughness.

2.2 Pavements

Pavement plays a significant role in social and economic development (TAC, 2014). It is one of the main critical investment operated by provincial, territorial, and municipal governments (CNC *et al*., 2015). Canada spent approximately 12 billion dollars annually on pavements as indicated by Public Works Canada (Smith, Tighe, & Fung, 2001).

Roads are exposed to climatic changes and heavy truck loads which as a consequence affect their serviceability and reduce their lifespan (TAC, 2014). In cold regions, in particular countries exposed to snow, ice, and frost heave during a significant period of the year, Freeze-Thaw Cycles have a drastic impact on the pavement structure (Salour & Erlingsson, 2012). According to White and Coree (1990) 60% of the deterioration occurs during the thaw period on the AASHTO road test (Doré *et al*., 2005). A research carried out by Transport Quebec (Saint-Laurent & Corbin, 2003) was focused on the effects of load circulating during the spring period on road deterioration. The scope of such research was to estimate the effect of removing the weight restrictions on maintenance costs. Transport Quebec reported 30% to 85% of all annual roads damage occurs during the spring thaw

period (Doré *et al.*, 2005). Governments set regulations on public roads to preserve pavements from deteriorations, increase pavement life, and saving new road budgets.

Table 2.1 shows the cost savings associated with load restriction practices during the critical period for several countries. Reduced axle weight values, impact pavement rehabilitation on roads experiencing frost deterioration and explain the significant cost surveys observed in the table. Cost varies from one country to another because of the differences on the annual daily traffic and the road sensitive to frost heave. Such surveys range between 40% to 92% with a mean of 79% (C-SHRP, 2000).

Table 2-1 Cross-Country Comparison of Pavements (C-SHRP, 2000).

Country	Percent of pavement That experience	Average annual daily traffic	Cost of a severe winter with load restrictions	Cost of a severe winter without	Associated cost saving of load restrictions

	frost and heave	(AADT)	(CAD million)	load restrictions (CAD million)	(percent)
Bulgaria	25%	2250	$300	$3750	92%
CSFR[1]	30%	2700	$450	$3450	87%
Hungary	40%	2900	$450	$4650	90%
Poland	15%	2240	$600	$2400	75%
Romania	50%	2700	$900	$6600	86%
Yugoslavia	45%	2100	$1350	$8100	83%
France	20%	4900	$7200	$12000	40%
Average					79%

1. CSFR (Czech and Slovak Federative Republic).

Table 2.2 shows an increase in the percentage of pavement lifespan when applying load restriction in the United States (C-SHRP, 2000). In a study done by The United States Federal Highway Administration (FHWA), it was found that when load restrictions of 20% are imposed, the pavement life span can be expected to increases by 62%. The load imposition influences on pavement lifespan as well as servicebility.

Table 2-2 Load Reduction versus Lifespan (C-SHRP, 2000).

Pavement load restriction during thaw	Expected pavement life increase
20%	62%

30%	78%
40%	88%
50%	95%

According to the USA practices, all Canadian provinces have issued public orders to restrict truck loading during the spring thaw period. This step aims to reduce the permanent deterioration of pavements by diminishing the axle loads (C-SHRP, 2000). **Table 2.3** presents the allowable loads under basic regulations and the spring load restrictions for different axles accommodated by Canadian provinces.

Table 2-3 Comparison of Basic and Seasonally Restricted Loads in Canada (C-SHRP, 2000).

Province	Allowable Weights Under Basic Regulations				Spring Load Restrictions			
	Tractor		Trailer		Tractor		Trailer	
	Steering	Drive	Tandem	Tridem	Steering	Drive	Tandem	Tridem
British Columbia	5500 kg	9100 kg	17000 kg (1.2 to 1.85m)	24000 kg (2.4 to 3.7m)	• Restrictions imposed only when and where needed through engineering judgment • Overload permits suspended for numbered highways • Other highways restricted at 70% or 50% of basic axle weight (steering axle exempted)			
Alberta	5500 kg	9100 kg	17000 kg	23000 kg (3.05 to 3.6m)	• 90%, 75% or 50% of basic axle weights			
					Not Restricted	8190 kg (90%) 6825 kg (75%)	15300 kg (90%) 12750 kg (75%)	21600 kg (90%) 18000 kg (75%)
Saskatch-ewan	5500 kg	8200 kg	14500 kg	20000 kg	• Reduction of load per tire from 10 kg/mm width to 6.25 kg/mm width to a maximum load of 1650 kg per tire • Some primary highways are downgraded to secondary highways during May and June			
					Not Restricted	6600 kg	13200 kg	19800 kg
Manitoba	5500 kg (A1 Hwys)	9100 kg (A1 Hwys)	16000 kg (A1 Hwys) (1.0 to 1.85m)	23000 kg (A1 Hwys) (3.05m)	• No restrictions to primary system or gravel roads • Steering axle not restricted • For other axles: • Level 1 (beginning of thaw for 14 days):			

<table>
<tr><td rowspan="3">Province</td><td colspan="4">Allowable Weights Under Basic Regulations</td><td colspan="4">Spring Load Restrictions</td></tr>
<tr><td colspan="2">Tractor</td><td colspan="2">Trailer</td><td colspan="2">Tractor</td><td colspan="2">Trailer</td></tr>
<tr><td>Steering

5500 kg
(B1 Hwys)</td><td>Drive

8200 kg
(B1 Hwys)</td><td>Tandem

14500 kg
(B1 Hwys)
(1.0 to 1.85m)</td><td>Tridem

20000 kg
(B1 Hwys)
(3.05m)</td><td>Steering</td><td>Drive</td><td>Tandem</td><td>Tridem</td></tr>
<tr><td colspan="8">• A1 highways 90% of basic load
• B1 highways 95% of basic load
• Level 2 (imposed 14 days after Level 1 and removed 1 week before removal of Level 1):
• 65% of basic load</td></tr>
<tr><td>Ontario</td><td>5000 kg</td><td>10000 kg</td><td>17200 kg</td><td>23000 kg</td><td colspan="8">• Primary network not restricted
• Restrictions on some secondary provincial highways up to 50% of basic load
• Commercial vehicles not to exceed 5000 kg
• 2-axle tanker truck not to exceed 7500 kg/axle
• Maximum of 5 kg/mm tire width</td></tr>
<tr><td>Quebec</td><td>5500 kg</td><td>10000 kg</td><td>18000 kg</td><td>21000 kg
to
26000 kg</td><td>5500 kg</td><td>8000 kg</td><td>15500 kg</td><td>18000 kg
to
22000 kg</td></tr>
<tr><td rowspan="2">New Brunswick</td><td>5500 kg</td><td>9100 kg</td><td>18000 kg</td><td>21000 kg
(2.4 to 3.0m)
23000 kg
(3.0 to 3.6m)
26000 kg
(3.6 to 4.8m)</td><td colspan="8" rowspan="2">• Three restriction levels:
• All-weather highways, arterials and most collectors allow 100% of basic load
• Specific collectors and locals allow 90% of basic load
• All other highways allow 80% of basic load
• Tolerance removed for all levels</td></tr>
<tr><td colspan="4">Tolerance 500 kg/axle</td></tr>
<tr><td rowspan="2">Prince Edward Island</td><td>5500 kg</td><td>6800 kg</td><td>13500 kg</td><td>18000 kg
(<3.6m)
19500 kg

(>3.6m)</td><td colspan="8" rowspan="2">• All-weather highways, Trans-Canada arterials and some collectors allow 100% of basic load
• Other highways allow 75% of basic load
• Tolerance removed during thaw</td></tr>
<tr><td colspan="4">Tolerance 500 kg/axle</td></tr>
<tr><td rowspan="2">Nova

Scotia</td><td colspan="4" rowspan="2">• Combination 50000 kg + 500 kg/axle tolerance
• 5-axle Semi-trailer 41000 kg + 2500 kg tolerance

(Schedule C highways and some arterials and collectors)
• Other highways 38500 kg gross vehicle + 500 kg/axle tolerance</td><td colspan="8">• Tolerance removed during thaw
• Max. gross weight 12000 kg for buses</td></tr>
<tr><td colspan="2">Not Restricted</td><td colspan="2">6500 kg</td><td colspan="4">12000 kg</td></tr>
<tr><td>New-foundland</td><td colspan="4">No formal policy
9100 kg Single, 12000 kg Tandem</td><td colspan="8">• Arterial and collector roads are all weather
• Local roads monitored and restricted as needed</td></tr>
</table>

2.3 **Freeze Thaw**

Road networks and pavement layers in cold regions are exposed to different environment conditions throughout the year. Pavement layers face subzero temperatures during the

winter season which last for an extended periods of time, this results in frost penetration in all layers: surface layer, base layer, subbase layer, and subgrade soil layer. Accumulated water can come from lateral moisture transfer; the capillary force that rose water from the water table, rainfall infiltration through surface cracks and joints (Salour & Erlingsson, 2012).

Water forms ice lenses in the pavement structure; layers. After that, in the spring season, water starts to melt down and transform back to a liquid phase in the phenomena called spring thaw cycle. In this stage, the pavement structure layers are exposed to relatively high moisture contents, which diminish the shear strength and loss of internal friction forces between the aggregates. Consequently, pavement loses its bearing capacity, subgrade becomes considerably softer, and a decrease in stiffness occurs. Also, the Hot Mix Asphalt layer experiences excessive fatigue damage owing to loss of support of the underneath layers (Salour & Erlingsson, 2012).

2.4 Effect of Freeze Thaw-Cycle on Pavements

A research by Salour and Erlingsson (2012) showed that a loss in stiffness of 63% in the subgrade layer and 48% in granular layers may happen during the spring thaw season in contrast to the stiffness values obtained in summer from falling weight deflectometer (FWD) measurements (Yi, Doré, & Bilodeau, 2016). **Figure 2.1** demonstrates the changes in overall stiffness of pavement in cold regions. The pavement stiffness in winter has larger values as compared to summer, autumn, and spring. It is clear that thawing has an adverse impact on pavement stiffness. As seen on **Figure 2.1** a sharp reduction in pavement stiffness and fatigue occur during the thawing period.

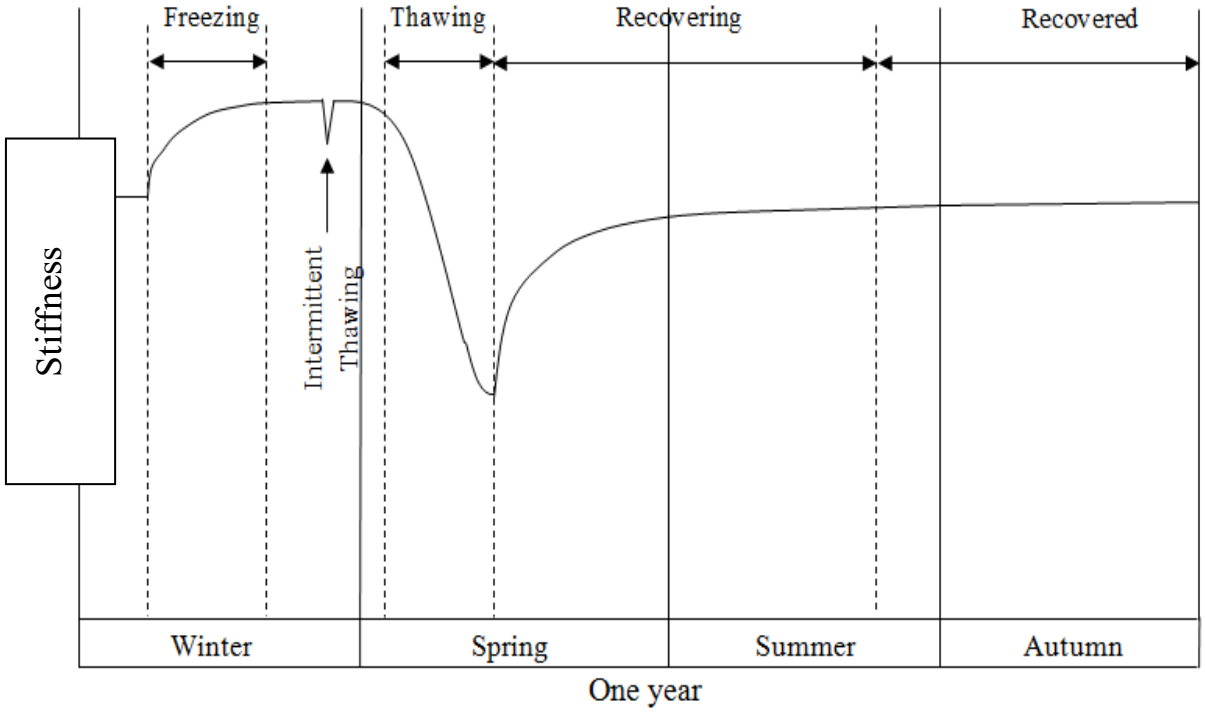

Figure 2-1 Schematic view of pavement stiffness variation due to freezing and thawing (Salour, 2015)

According to Doré and Savard (1998) the freeze-thaw cycle is the main cause of fatigue damage in Québec, Canada (Doré & Zubeck, 2009). The functional condition of a highway can be typified by three main characteristics: rutting, skid resistance, and surface roughness. The freeze-thaw cycle is deemed as one of the main deformation components of the pavement structure and affects rutting and the pavement smoothness (Doré & Zubeck, 2009).

Water iced in pavement layers and lead to an increase in volume, particularly in the soil. This increase in size creates an upward movement in the top bitumen layer and result in transverse expansions. When frost heave condition begins, typically iced water melts down and cannot drain smoothly throughout the pavement. Therefore, subgrade soil normally will have excessive moisture content. Susceptible distresses in the form of distortions, swelling, longitudinal cracking, transverse cracking, edge cracking, centerline

cracking, and rutting will occur (Mahoney, Rutherford, & Hicks, 1987) . This excess water content increases the tensile strain and the fatigue cracking sensitivity, also, reduces the resilient modulus of the flexible pavement layers under traffic loads (Yi *et al*., 2016). The reduction of the elastic modulus for unbound materials and subgrade soils during the thaw period, relative to summer modulus is approximately equal to 36% for granular base, 30% for subbase, and 54% for subgrade soil (Doré & Zubeck, 2009)

Figure 2.2 is an example of typical pavement deflection changes throughout the year caused by winter freezing and spring thawing. **Figure 2.2** shows pavement damage as a result of thaw weakening (Mahoney *et al.*, 1987). Indeed, deteriorate pavement will cause an infliction and reduction in road service life as well as providing a poor quality of ride for commuters (Schaus & Popik, 2011).

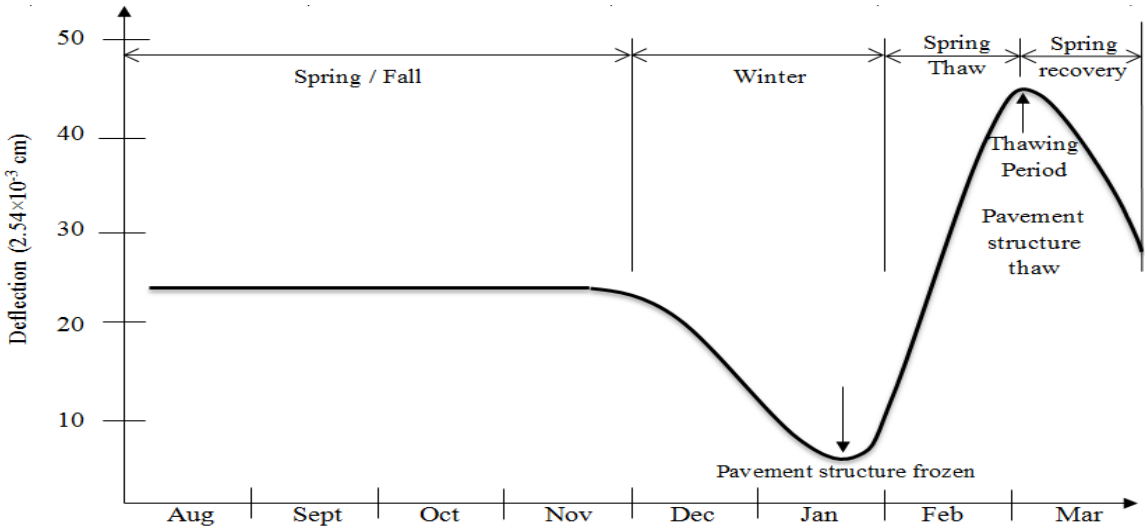

Figure 2-2 Typical pavement deflection, seasonal changes, modified (Mahoney *et al*., 1987).

Figure 2.3 was taken on March 17, 2017 at the highway 20, Montreal Quebec. It shows clearly that the pavement exposed to freeze thaw cycle. Pavement roughness deteriorated; pothole, cracks, and rutting were occurred.

Figure 2-3 Freeze-Thaw Damage on highway 20 near exit 68

2.5 Seasonal Weight Restriction in Canada and the World

In the thawing period, pavement is exposed to fatigue damage due to saturation in its structure layers. Thus, pavements need to be protected through imposed Seasonal load Restrictions (SLR) (Aho & Saarenketo, 2006). Seasonal load restrictions apply during the time to the structure needs drain trapped water, recover, and be protected from fast deterioration. When the thawing starts and the pavement lose its stiffness, seasonal weight restriction should be placed (Ovik, Siekmeier, & Van Deusen, 2000).

Restrictions are placed based on data compiled throughout significant investigations on pavement behavior. This type of policy aids manage and improve road conditions during the spring thaw weakening period (Yi *et al.*, 2016). A study was conducted in Washington State has placed load restrictions depends on the pavement stiffness. The restrictions should

be imposed when the pavement stiffness drops below 40% to 50% of their fully recovered values. The restrictions might be removed after pavement stiffness recovers to above 40 to 50 percent (Steinert, Humphrey, & Kestler, 2005). Therefore, an accurate prediction for the exact critical time of thawing with proper measurement for the pavement condition should be used to improve the strategies of seasonal load restriction imposition (Ovik *et al.,* 2000).

The period of thaw for a typical pavement structure depends on soil type, air temperature, moisture, thermal properties, drainage, solar radiation, and the location of the site (Crowder & Shalapy, 2008). The exact time for SLR at when to impose and remove, is subjected to several components: traffic flow, pavement structure, land topography, drainage condition, air temperature, frost depth, and soil type (Ovik *et al*., 2000).

In general, Canadian provinces and many States count on engineering experience and visual observation to decide when to impose and remove SLRs. However, visual observations include rapid deterioration of the surface layer, water seeping through cracks upward as traffic loads are applied, and soft shoulders (Ovik *et al*., 2000).

For example, in Manitoba province, the length of SLRs is associated with the calendar day, regardless of the thawing condition. This typically last ten weeks in southern Manitoba and six to eight weeks in northern Manitoba. However, if there is no significant thawing, the imposition might be delayed (Ovik *et al.*, 2000).

Table 2-4 Seasonal load restriction imposition start and end dates in Canadian provinces (C-SHRP, 2000).

Province	Start of SLR	End of SLR	Determination of restriction
British Columbia	Mid of February	Mid of June	frost probes, deflections, historical data
Alberta	30cm of thaw	from FWD testing	FWD
Saskatchewan	2nd or 3rd week in March	maximum 6 weeks	Benkelman Beam
Manitoba	Northern zone: April 15	May 31	Benkelman Beam
	Southern zones: March 23		
Ontario	first Monday in March in south Regions	Mid of May	N/A
Quebec	North: March 24	May 25	frost probes
	Central: March 6	May 12	
	South: March 21	May 19	
New Brunswick	2nd or 3rd week in March	mid or end of May	Dynaflect testing
Prince Edward Island	March 1	April 30	Dynaflect testing
Nova Scotia	South: March 2	April 24	Dynaflect testing
	Central/North: March 2	April 27	
Newfoundland	February	April	N/A

N/A no data available

Table 2-5 Seasonal load restriction imposition start and end dates in some Europe countries (Levinson *et al*., 2005)

Country	Start of SLR	End of SLR	Determination of restriction
Finlad	April	May	FWD, experience
Iceland	30cm of thaw	N/A	frost depth measurements
Sweden	April	May	FWD, frost depth measurements, experience
Norway	past: 5-15cm of thaw	min. 90% of summer bearing capacity	FWD, frost depth measurements
	present: prediction that pavement will break down	4-8 weeks after imposing	

N/A no data available

Table 2-6 Seasonal load restriction imposition start and end dates in some Sates (Levinson *et al.*, 2005)

State	Start of SLR	End of SLR	Determination of restriction
North Dakota	March 15	June 1	Deflection measurements and experience
South Dakota	February 28	April 27	deflection measurements and experience
Iowa	March 1	May 1	Road Rater and experience
Wisconsin	March 10	May 10	deflection measurements and experience
Michigan	Early March	Late May	experience

State	Start of SLR	End of SLR	Determination of restriction
Minnesota	March	May	design testing and experience

Canadian provinces, several states, and nordic coountries in Europe use SLR to prevent pavement structure from detorioration during spring season. The quality of data available to characterize the road structural and functional condition could also be used to create a sustainable pavement structure, and improve SLR prediction time. Typically, SLR last for eight weeks, starting in late February or early march till the end of April or begin of May. Different methods might be utilized; their selection depends on municipal government decision to determine when to perform and remove SLRs. It could be one of the following methods or a combination of them:

1. Setting the date by the calendar each year.
2. Engineering judgment.
3. Pavement history.
4. Pavement design.
5. Visual observations, such as water seeping from the pavement.
6. Restrict travel to night-time hours (appropriate for unpaved roads only).
7. Daily air and pavement temperature monitoring.
8. Frost depth measurement using drive rods, frost tubes, and various electrical sensors.
9. Deflection testing. (Ovik *et al*., 2000).

In the following paragraph, the influential methods that commonly used for the seasonal load restriction imposition and timimng have been briefly discussed (C-SHRP, 2000).

2.6 Methods for Timing Load Restrictions

2.6.1 Frost Tube

In order to obtain the period of frost depth, tools can be used to measure frost such as drive rods, various electrical sensors, or frost tubes. Such tools will acquire the magnitude and duration of temperatures, below or above freezing at the ground surface, which will impact the frost and thaw penetration (Ovik *et al*., 2000).

Frost penetration depth (FPD) gradually progresses along in a pavement structure layers with an increase in frost period. It is always higher at the beginning of the freezing period and then decreases regularly. Thus, it is defined as a function of square root of frost time with a constant, given a distance measured in meters (Yi *et al.*, 2016).

$$FPD = 0.0449 \sqrt{t} \qquad (R^2 = 0.9639) \qquad (1)$$

Where **FPD** is frost penetration depth (meters) and,

t is freezing time (hours).

2.6.2 Measurement of Daily Air and Pavement Temperature

Data gathered from weather forecast monitoring stations for the past few years improve the reflection of frost and heave periods on the pavement structure (C-SHRP, 2000). Whereas, pavement temperature probes could be installed at different depths to represent the accurate layer temperature, and to enhance the understanding of pavement condition (Salour & Erlingsson, 2012).

A research was conducted by Farhad and Sigurdur (2012) in the south of Sweden on the behavior of pavement during the spring thaw. They observed the variation in the pavement profile temperature and moisture content during thaw and recovery periods. The results are reported in **figure 2.4**.

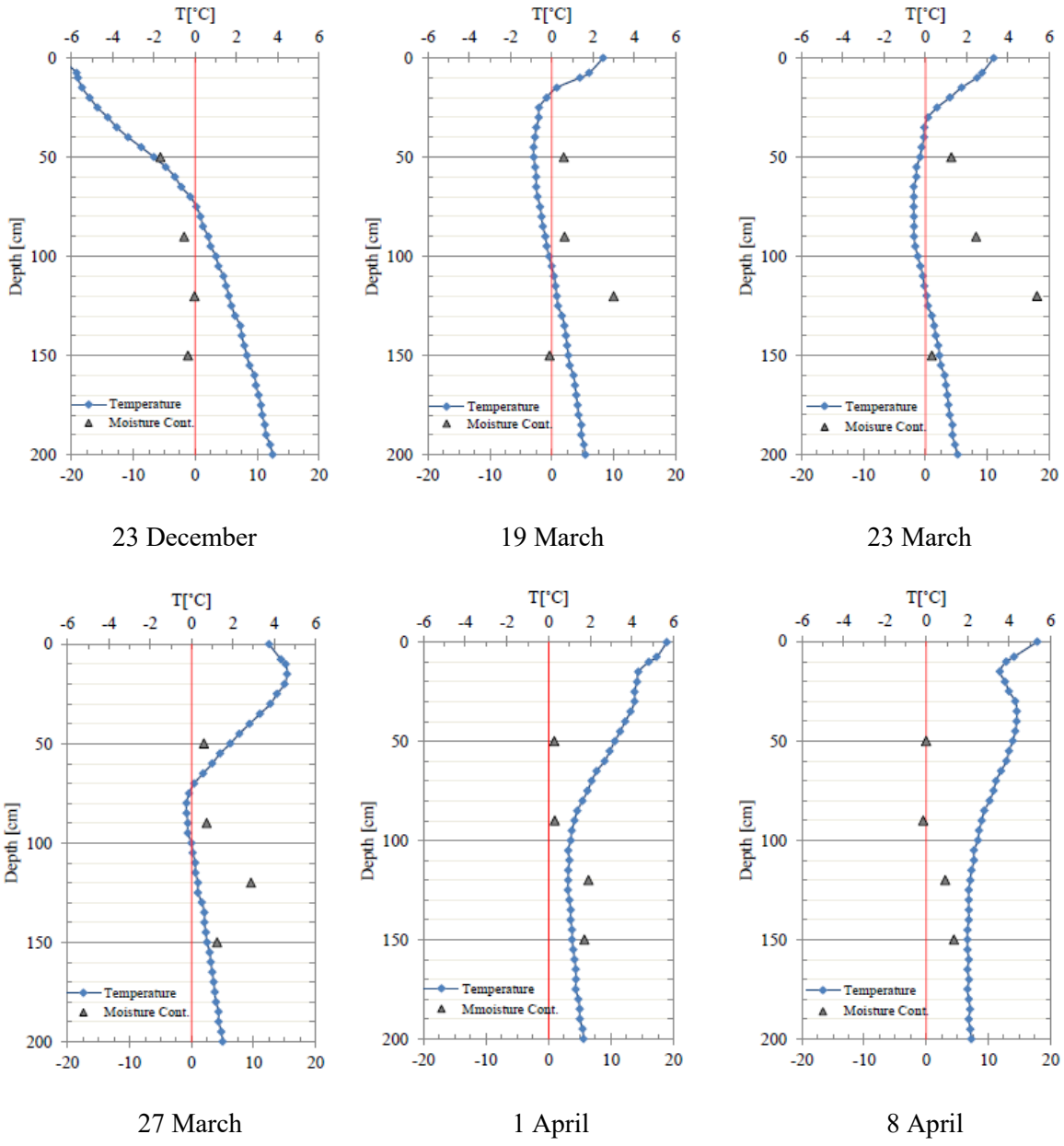

Figure 2-4 Pavement profile temperature and moisture content during thaw and recovery period (Salour & Erlingsson, 2012).

On December 23rd, the moisture content was below zero temperature, as a result of frozen pavement. After compiled data, thawing started and the moisture content increased corresponding with the pavement temperature. The moisture content gradually reduced towards the end of spring as the water drained out from the pavement (Salour & Erlingsson, 2012). Measurement of air daily and pavement temperature aids to predict the perfect time to impose and release the load restrictions.

Moreover, The Washington Department of Transportation (WSDOT) predicted the thaw period after extensive significant research. They synchronize a relation between the average air temperature and the thaw depth in the pavement structure. This relation incorporated in simple equations called the thawing index TI and the freezing index FI (Ovik *et al.*, 2000).

1. $TI = \Sigma\ (Tmean - Tref)$ (2)

Where Tmean = mean daily temperature, in °C = 0.5(T1 + T2), and

T1 = maximum daily air temperature, in °C,

T2 = minimum daily air temperature, in °C.

And Tref = reference freezing temperature that varies as pavement thaws, in °C.

2. $FI = \Sigma\ (0°C - Tmean)$ (3)

"The TI is defined as the positive cumulative deviation between the mean daily air temperature and a reference thawing temperature for successive days. While the FI is defined as the positive cumulative deviation between a reference freezing temperature and the mean daily air temperature for successive days" (Ovik *et al.*, 2000).

2.6.3 Falling Weight Deflectometer

Falling weight Deflectometer (FWD) is a nondestructive, direct method. It is a device most widely used to evaluate the pavement structure. The impact of pulse wheel load on pavement

surface simulates the load equivalent occurred by the FWD plate (Barman & Pandey, 2008). It is used to acquire the mechanical response of pavement structure layers under a test plate load (Doré & Zubeck, 2009). In 1982, the FWD device costed around 60,000$ (Eagleson *et al.,* 1982), while recently, the price tag of a FWD has been increased drastically to 150,000$. Developing countries and small municipalities can't afford this equipment, they rely on more practical and cheaper equipment (Hanson, Cameron, & Hildebrand, 2014).

A modern FWD contains three main components: the loading unit that produces the load impact on a circular plate by dropping a defined falling weight from a certain height. Second, the measuring units which consist of specific deflection sensors called geophones. These sensors record the pavement surface deflection at a known distance away from the loading plate. Finally, the data acquisition systems (Salour, 2015).

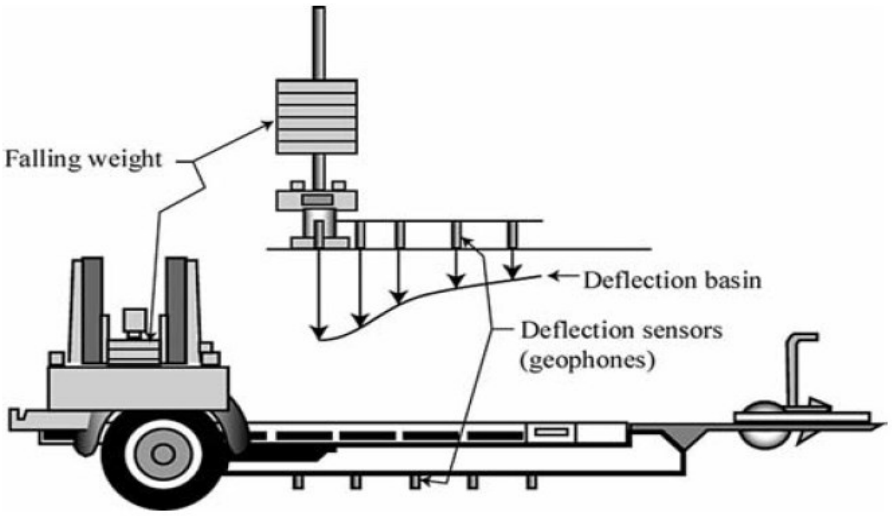

Figure 2-5 Sketch view of Falling Weight Deflectometer and its parts (Doré & Zubeck, 2009)

From the data acquired by a FWD one can estimates various deflection indices such as the Surface Curvature Index (SCI), the Base Damage Index (BDI), and the Base Curvature Index (BCI) and therefore estimate an indication of the mechanical behavior of the

pavement structure. These parameters can be used during different points on time to evaluate a pavement structure exposed to different seasonal conditions (Talvik & Aavik, 2009). Deflections recorded near the center of the load plate indicate the material properties of the subgrade soil while the strength of the pavement layers can be measured at a sufficient distance away from the plate load center (Salour, 2015).

Table 2-7 Shows deflection basin parameters and their equations.

Deflection basin indices	Equation	Description	References
Surface Curvature Index (SCI)	$SCI = d_0 - d_{300}$	characterizing stiffness of the top layer (0-200mm)	(Doré & Zubeck, 2009)
Base Damage Index (BDI)	$BDI = d_{300} - d_{600}$	characterizing condition of the base layers	(Talvik & Aavik, 2009)
Base Curvature Index (BCI)	$BCI = d_{1200} - d_{1500}$	characterizing condition of the top part of the subgrade (800-1000mm)	(Talvik & Aavik, 2009)

Note: all the (d)s in the Equation column are measured deformations at the distance of 0, 300,600, 1200, and 1500 mm from the center of the loading plate test.

The FWD is a perfect tool to evaluate seasonal variation conditions in pavement structure material and soil, that is compulsory to support seasonal deterioration assessments in pavement design and analysis (Doré & Zubeck, 2009).

Figure 2.6 (1994) illustrates the variation in the elastic modulus and seasonal response of pavement layers as measured using deflection testing on Highway 352 in Quebec,

Canada. **Figure 2.6-*a*** shows the pavement structure layer thicknesses as well as the frost and thaw depths in specific months during the year. Whereas, **Figure 2.6-*b*** illustrates the variation of the modulus of the hot mix asphalt layer. **Figure 2.6-*c*** demonstrates the variations in elastic modulus of base, subbase, and subgrade soil layers. The test showed that the elastic modulus measured by FWD during the thaw period has decreased compared to summer modulus. It was found that for granular base, the elastic modulus reduced by 36%, for the subbase by 30%, while for the subgrade soil by 54% (Doré & Zubeck, 2009).

The separation in pavement structure layers into frozen, thawed, saturated, and thawed drained behavior during the spring thaw season could possibly change the response of pavement layers to the FWD test and affect their elastic modulus. Thus, one test peer week should be considered during the first month in spring. If the thaw is progressing rapidly or detailed assessment is needed, more than one test peer week must be taken (Doré & Zubeck, 2009).

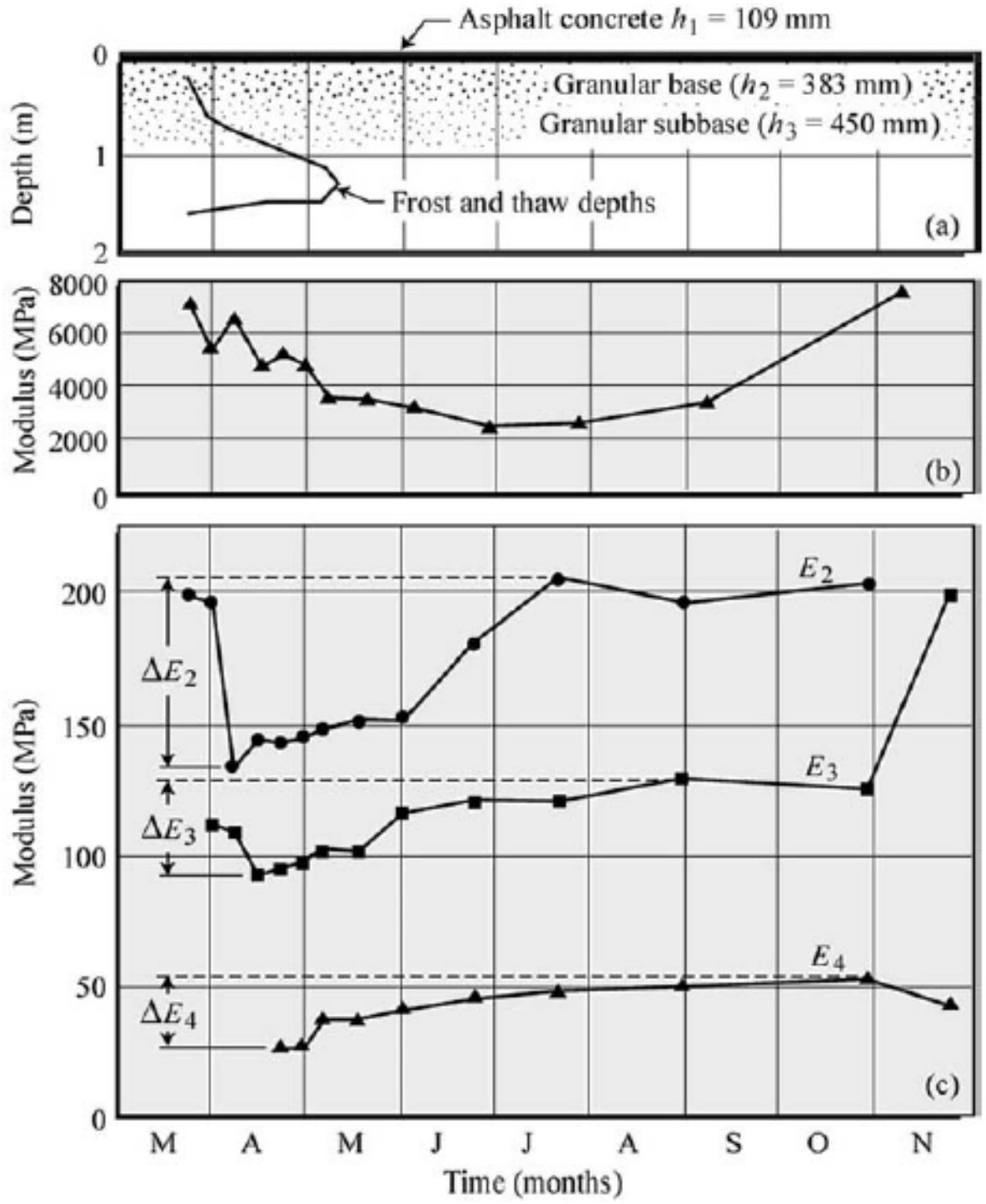

Figure 2-6 Seasonal response of pavement layers as measured by deflection testing (Doré & Zubeck, 2009)

2.6.4 Indirect Methods for Load Restriction Imposition

Transportation agencies and municipalities have supported various methods to set the start and end dates of SLR imposition. Indirect methods usually apply where financial constraints are found. Agencies without a FWD usually utilize visual observation of the surface layer and water seeping through cracks upward. They follow fixed scheduled dates according to predefined calendar days. Visual observations regardless of thawing condition are still common practice in northern countries. Also, engineering experience is crucial to determine the beginning and length of the SLR period as well as weather databases for developing prediction models (Asefzadeh *et al.*, 2016).

2.7 Pavement Condition

Adequate evaluation of pavement condition is required for modern pavement management as it is an essential asset of the highway infrastructure. Pavement indicators serve to give an indication of the serviceability and physical conditions of road pavements, also, help evaluate its performance. Indicators serve to scale roughness, friction, distress and any other maintenance problems that pavement engineers may need to face (Shah, *et al.,* 2013).

Pavement condition may be quantified with two different types of condition indices. Measured condition indexes which are gathered by physical measurements (such as roughness) and mathematical expressions. Estimated condition ratings are essential on pavement evaluation. They are based on observed physical condition of pavement structure (Attoh-Okine & Adarkwa, 2013).

In pavement management fields, there are several different performance indices that can be utilized. Their selection depends on the data availability and the desirable use of

performance model; such as International Roughness Index (RI), Present Serviceability Index (PSI), Pavement Condition Index (PCI), Pavement Quality Index (PQI), Pavement Rating Index (PRI), Surface Distress Index (SDI) (Shah *et al.*, 2013).

The European Cooperation in the Field of Scientific and Technical Research has defined the need to count with a Pavement Condition Indicator as "a superior term of a technical road pavement characteristic (distress) that indicates the condition of it (e.g. transverse evenness, skid resistance, etc.). It can be expressed in the form of a Technical Parameter (dimensional) and/or in the form of an Index (dimensionless)" (Antunes *et al.*, 2008).

Pavement roughness is the most universally accepted index for pavement condition and will be discussed in the next section and used in this research.

2.8 **Pavement Roughness**

Roughness of a pavement structure is deemed as one of the most important factors in a pavement management system. It impacts not only the pavement performance but is associated with vehicle operating cost, driver comfort, and road safety (Haas, Li, & Tighe, 1999).

There is no one single definition of pavement roughness. The word roughness has many approaches including qualities such as ride quality and drainage that are generally unrelated to each other. It is a condition experienced by the operator of vehicle and its passengers. However, the American Society of Testing and Materials has defined pavement roughness as; the severity of variation on the vertical dimension, also, the deviation and irregularity of a pavement surface from the complete smoothness which affect commuter quality because

of the dynamic movement and the vehicle dynamics (Sayers & Karamihas, 1998). Also, it has been defined as a deformation of the pavement surface that result in unpleasant ride for the commuters (Mactutis, Alavi, & Ott, 2000).

Environment conditions, irregularities in paved constructions, and traffic loads may affect the pavement roughness. During the process of built-in construction surface for a pavement, distortion roughness may occur. Though, new pavement could experience roughness even before it is open to use for public. Yet, environment conditions and traffic loadings are considering the main cause for increases roughness. Roughness is divided into two criteria: long-wavelength and short-wavelength. Environment processes and pavement layer materials normally the base cause of long-wavelength roughness. While, the short-wavelength roughness normally caused by depression and cracking (Hu, 2004).

2.8.1 Pavement Roughness Evaluation

In the 1920s, pavement roughness evaluation was first recognized as a crucial element of a road pavement condition. Late after, pavement performance concept was developed at the AASHTO Road Test. Some of roughness measuring methods consume time, have limit to measure short sections of pavements, and are also expensive. For example, the most direct technique for measuring the profile section is with precision rod and level survey (Hu, 2004).

There are different ways for road surface condition data to be obtained. Intensive human intervention technique with low speed considers visual inspection for pavement assessment. In contrast, other techniques that need expensive measurement equipment's with high skillful operators, for example, sophisticate profilers (Douangphachanh & Oneyama, 2013).

In general, roughness measurement systems process may divide and consist of two main steps:

- **Collect data in the field** which can be obtained by several methods.
- **Data analysis** which can be processed, (after gathering data from the first step) by computer software to extract the desire road section that has been tested.

2.8.1.1 Profilometer Method to Estimate Pavement Roughness

There are two methods of collecting data to estimate pavement roughness. Profilometer-type method and response-type method (Bennett, 1996). Profilometer is an instrument used to collect data on the road pavements, by producing a sequence of numbers that reflect pavement roughness data. Certain ingredients must be provided for any profiler to function. These components are very important and combined together in different ways based on the profiler design system (Sayers & Karamihas, 1998). The ingredients are:

1. Longitudinal intervals.
2. Referral elevation.
3. Known height relative to the reference elevation.

General Motors Research Laboratories developed the profiler system in the 1960s. They merge the old dipstick and rod level into one measurement system known as inertial profiler. Inertial profiler detects the vertical displacement acceleration by an accelerometer backed in the vehicle. Compiled data processed through algorithms in order to transfer vertical movement to inertial reference that describes the instant height of the accelerometer in the host vehicle. The distance between the accelerometer and the pavement surface is the height relative to reference. This height measured without direct contact to pavement

surface. Instead, it uses laser transducer, ultrasound waves, or infrared sensor. Finally, the longitudinal intervals are recorded through the vehicle speedometer. Hence, to start collecting data by a Profiler, vehicle must be moving on the pavement section desired (Sayers & Karamihas, 1998).

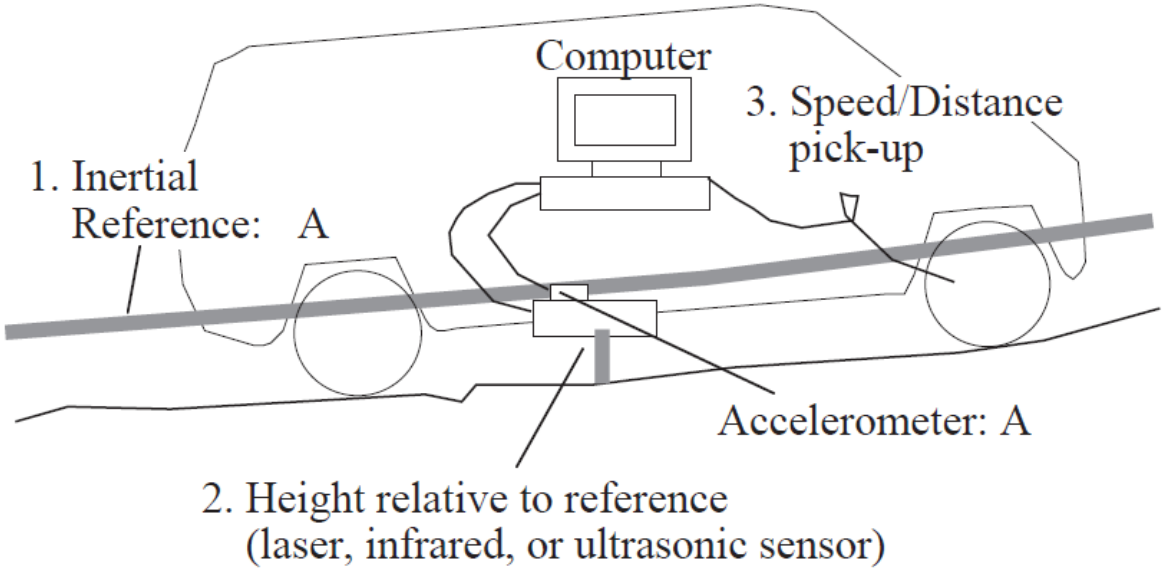

Figure 2-7 Sketch of inertial profiler (Sayers & Karamihas, 1998)

2.8.1.2 Response-Type Method to Estimate Pavement Roughness

Pavement roughness irregularities can be detected by a device backed in a vehicle through a system called Response Type Method. The variation of the pavement elevation may record through measuring the vehicle chassis relative to the rear axle. Compiled data can then be used to produce International Roughness Index (RI). Usually, presents in units of meter per kilometer (m/km) or inches per miles (in/mi) (Bennett, 1996).

The response type records data on a large scope of road networks through dynamic movements to reach the final pavement condition database. Also, the sensor system used is very accurate comparing to other data collection unit (Katicha, El Khoury, & Flintsch,

2016). On the other hand, since data are not repeatable and cannot be comparable with other instruments, data obtained may differ from one vehicle to another even using the same system. The reason of these limitations is that vehicle responds differently to pavement undulations the shock absorber, spring elasticity, and tire inflation pressure. Thus, specific principles should have considered. Also, it is recommended for vehicles to be calibrated against roughness measure to ensure the accuracy, low cost, and valid results (Bennett, 1996).

2.9 International Roughness Index RI

An accurate characterization of road roughness in a longitudinal road profile is essential for road maintenance, to ensure ride comfort and safety, and to reduce dynamic load on a vehicle and pavement (Múčka, 2017). The International Roughness Index was first established and evolved out by the World Bank in Brazil in 1982. RI has been the most commonly used pavement indicator worldwide.

The following organization and profiler users have shared their experience in measuring RI values, Road Profiler User Group (RPUG), the Federal Highway Administration (FHWA), and the Highway Performance Monitoring System (HPMS) (Sayers & Karamihas, 1998). Its obligation is to measure pavement performance and ride quality. However, it is very correlated to overall pavement loading vibration level and to overall ride vibration level (Múčka, 2017).

The international roughness index is a computer-based virtual response-type system based on the response of a mathematical quarter-car vehicle model to a road profile. RI essentially is based on the simulation of the roughness response of a car travelling at 80

km/h. However, it expresses a relation between accumulated suspension vertical motion of a vehicle, and the distance travelled during the test (Múčka, 2017).

The International Roughness Index has become recognized and accepted around the world to measure surface condition (Haas *et al.*, 1999). The collected RI data presents pavement roughness in inches per mile (in/mile) or meter per kilometer (m/km). It can theoretically ranges from 0.0 for a very smooth surface to up of 10.0 for irregular pavement surface (Douangphachanh & Oneyama, 2013). There is no theoretical upper limit of RI values (Sayers & Karamihas, 1998).

Table 2.5 proposed by Viengnam & Hiroyuki, classifies the road roughness condition from good condition to bad based on RI values.

Table 2-8 RI Condition Index (Douangphachanh & Oneyama, 2013)

Pavement Condition	Average RI
Good	0≤RI<4
Fair	4≤RI<7
Poor	7≤RI<10
Bad	RI≥10

There are significant advantages of RI data which deemed it as a general indicator of pavement surface condition. Data gathered from RI can be compatible and compared with other data even from one country to another, stable with time, portable, and reproducible. Also, RI can be measured by any type of profiler since it is a characteristic of a true profile (Sayers & Karamihas, 1998).

2.9.1 Overall Changes in RI by Canadian Provinces

The table below illustrates the changes observed in RI values for newly constructed pavements during the as-built period and after seven years of use. Three provinces were considered. Their selection depended on the climate zone classification, where the freeze-thaw cycle impacts the RI values adversely (RI increase).

Table 2-9 Illustrates changes in average RI for three Canadian provinces (Haas *et al.*, 1999)

Location	Climate Zone	RI As-built in 1989/1990			RI in 1997			Δ RI
		Q_1	Q_3	Mean	Q_1	Q_3	Mean	change in 7 Years
Quebec	II	1.109	1.254	1.181	1.183	1.420	1.333	0.15
Manitoba	III	1.092	1.347	1.246	1.020	1.575	1.313	0.06
British Columbia	I	0.880	1.219	1.056	1.170	1.229	1.250	0.19

Hence: I for wet, low freeze zone. II for wet, high freeze zone. III for dry, high freeze zone.
Q_1 is the first quartile.
Q_3 is the third quartile.

The relatively small changes in RI values over time result from combination of traffic loads and climatic changes and capture only the first 7 years of pavements life. From the table above it is obvious that the RI in zone III observe the largest change on RI followed by zone II and zone I being last. The values reported serve only as a general indication as they missed changes during later points of the lifespan of the pavements. It is expected that older pavements in the province of Quebec will suffer larger RI variations over each freeze thaw cycle (Mactutis *et al.,* 2000).

2.9.2 Calculation of RI

The RI is calculated using the quarter-car model. It is an algorithm of differential equations that relate the vertical movement of a simulated quarter-car to a longitudinal road profile (Bennett, 1996). In particular, the RI can be computed by accumulated a relative displacement of the tire width respect to the frame of the quarter-car and dividing the results by the profile length, as shown in the next linear equation (Sayers, 1995).

$$RI = \frac{1}{L}\int_{0}^{\frac{L}{S}}(Zs - Zu)dt \qquad (4)$$

RI: International Roughness Index (m/km).
L: Profile length (km).
S: Simulated speed (80 km/h).
Zu: Time derivative of the height of the unsprung mass.
Zs: Time derivative of the height of the sprung mass.

The Root Mean Square (RMS) is another method that might be used to calculate the RI. The RMS method is a bit complicated in terms of it is a nonlinear equation with respect to absolute amplitude, unlike the previous equation. For instance, in the RMS method if the RI for a half (km) is 100 m/km, and for the other half is 200 m/km. Then the RI for 1 km will 158 m/km, while in the linear method, the RI will be the simple average of 150 m/km (Sayers, 1995).

CHAPTER 3

3 Methodology

3.1 Introduction

This chapter presents the process used for data acquisition and database preparation. The goal is to test if the progression of roughness can be used to monitor pavement rapid deterioration and hence serve to impose the load reduction factor and timing. Thus, the chapter has been divided into three main sections. First section presents the test segment description and location. The second section provides the steps needed to estimate the roughness data. In the third section, the database preparation is presented as well as the final approach to compare multiple time points.

3.2 Test Segment Description

This research has been based on data recorded on a segment of highway 20/ AutoRoute 20 (A-20) in the west part of Montrèal, Québec during nine months. This period of time was selected to encompass the whole environmental cycle from a freeze-thaw cycles perspective. Highway 20 is 453.1 km long and the studied section is about 8 km long; beginning immediately after the AutoRoute 720 toward the west to exit 60, (AutoRoute 13 north/32 Avenue – Laval, Mirabel Airport). The section was built in 1964 and funded by the ministry of transportation (de la Mobilité durable et de l'Électrification des transports Ministère des Transports, 2017a) . **Table 3.1** explains the road section including its average daily traffic (ADT) and trucks percentage as well as pavement type. The studied section is shown in **figure 3.1.**

Table 3-1 Road section details (de la Mobilité durable et de l'Électrification des transports Ministère des Transports, 2017b).

Road Section	ADT	Trucks %	Pavement type	Coating
A-20 west, from Turcot exchange to St-Pierre interchange	63,000 vehicle/day	8.1%	Flexible	. 230 mm coated
A-20 west, at the St-Pierre exchange	39,050 vehicle/day	6.6%	Mixed	. 190 mm concrete slab . 25 mm sealing cap . 50 mm coated
St-Pierre exchange to exit 60	68,440 vehicle/day	9.1%	Mixed	. 230 mm concrete slab . 25 mm sealing cap . 50 mm coated

ADT: average daily traffic

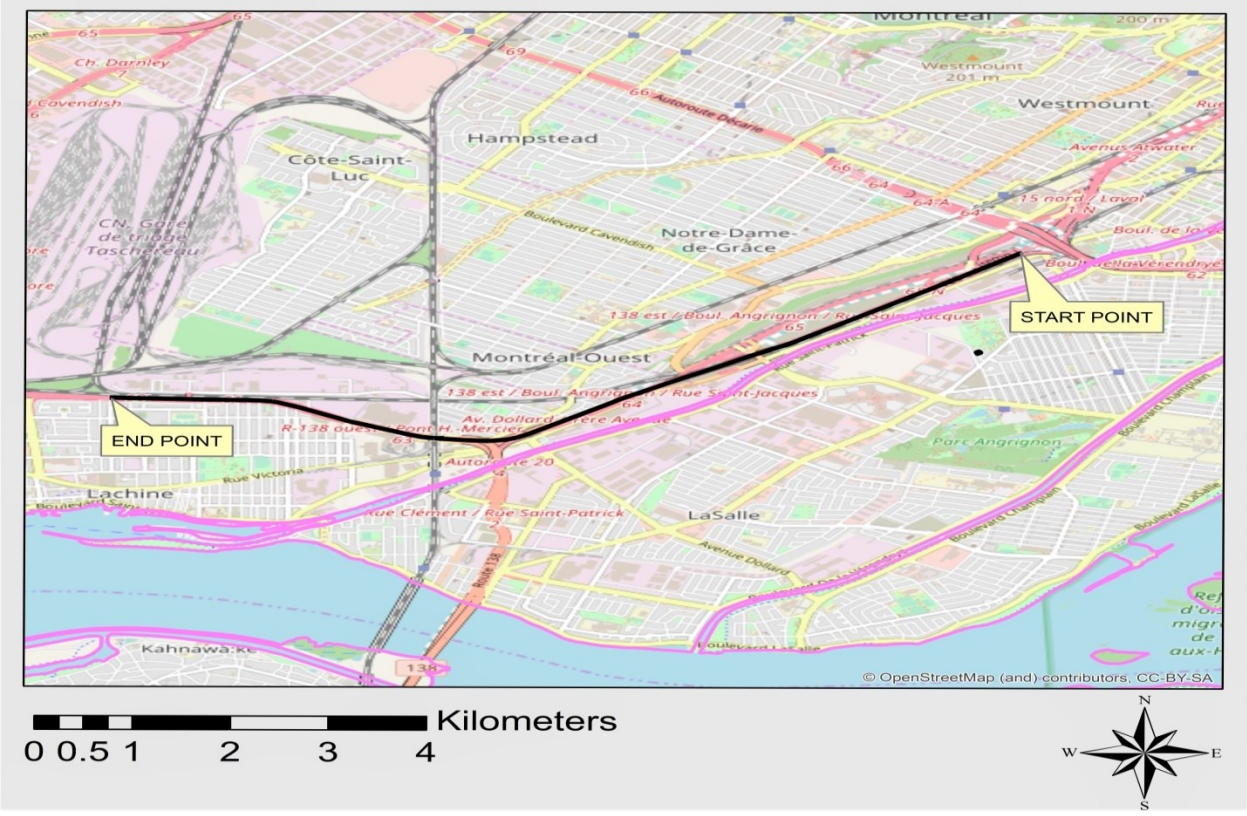

Figure 3-1 Spatial location of the tested road section (A-20), (ArcGIS Online).

3.3 Test Segment Location

The province of Québec has been divided into three zones in terms of frost and heave. Highway A-20 is located in zone one which has the first seasonal load restriction imposition. **Table 3.2** below provides the start and end dates followed by the government as well as the duration of the thawing for the three zones in Québec. In this research, the progression of roughness in zone one will be measured. The mean duration days of the thaw period since 1991 till 2016 for the zone one are 57.3 days. Basically, in Québec the frost duration is 147 to 218 days while the frost depth is approximately 1.2 to 3 m (Peter Múčka, 2017). **Figure 3.2** shows the three zones distribution in Québec with the allocation of A-20 in the red block in zone one (de la Mobilité durable et de l'Électrification des transports Ministère des Transports, 2017c).

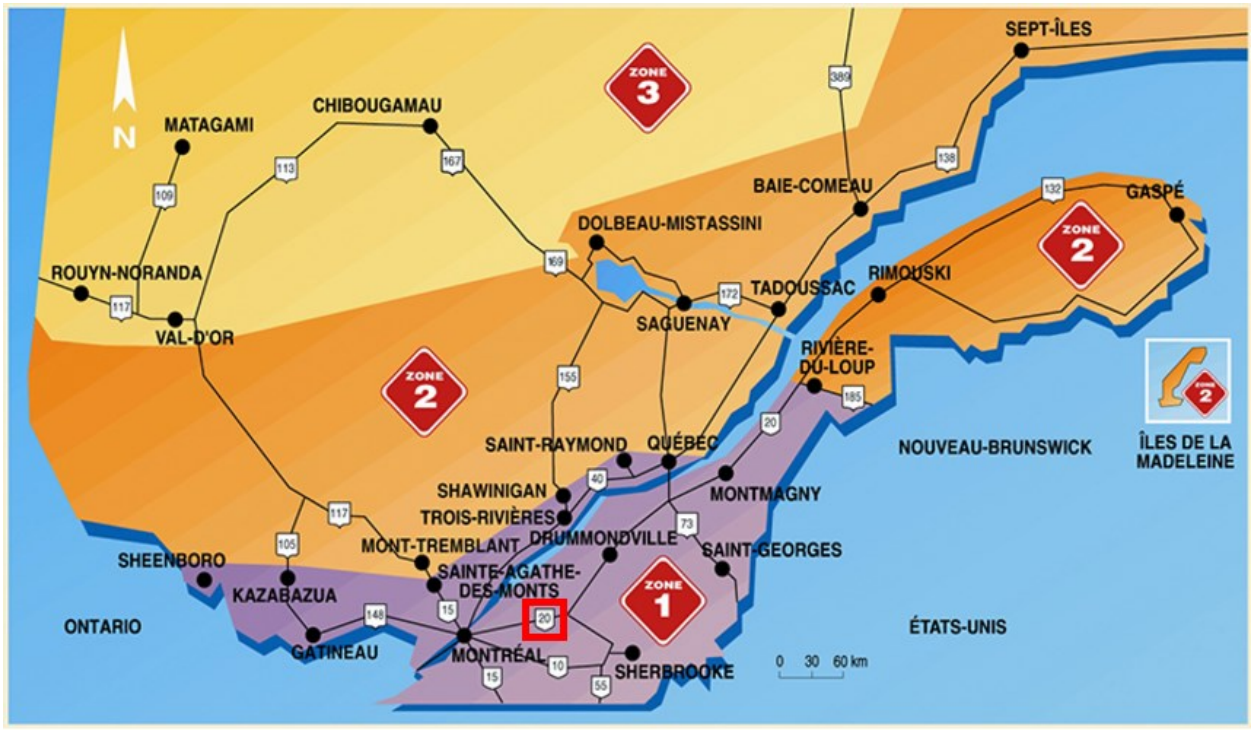

Figure 3-2 Thaw distribution zones in Québec (de la Mobilité durable et de l'Électrification des transports Ministère des Transports, 2017c).

Table 3-2 Thaw history from 1991 to 2017 in Québec (de la Mobilité durable et de l'Électrification des transports Ministère des Transports, 2017b).

Year	Zone 1			Zone 2			Zone 3		
	Start	End	Duration	Start	End	Duration	Start	End	Duration
1991	13 March	10 May	58 Days	20 March	17 May	58 Days	28 March	25 May	58 Days
1992	13 March	10 May	58 Days	20 March	17 May	58 Days	28 March	25 May	58 Days
1993	13 March	10 May	58 Days	20 March	17 May	58 Days	28 March	25 May	58 Days
1994	13 March	10 May	58 Days	20 March	17 May	58 Days	28 March	25 May	58 Days
1995	13 March	10 May	58 Days	20 March	17 May	58 Days	22 March	29 May	68 Days
1996	15 March	12 May	58 Days	21 March	19 May	59 Days	24 March	25 May	62 Days
1997	15 March	12 May	58 Days	21 March	19 May	59 Days	24 March	25 May	62 Days
1998	5 March	5 May	61 Days	5 March	12 May	68 Days	24 March	17 May	54 Days
1999	21 March	6 May	46 Days	21 March	15 May	55 Days	24 March	25 May	62 Days
2000	6 March	12 May	67 Days	21 March	19 May	59 Days	24 March	25 May	62 Days
2001	12 March	16 May	65 Days	19 March	16 May	58 Days	26 March	21 May	56 Days
2002	11 March	11 May	61 Days	18 March	18 May	61 Days	25 March	25 May	61 Days
2003	21 March	17 May	57 Days	24 March	24 May	61 Days	31 March	31 May	61 Days
2004	15 March	15 May	61 Days	22 March	22 May	61 Days	29 March	29 May	61 Days
2005	21 March	15 May	55 Days	28 March	21 May	54 Days	4 April	21 May	47 Days
2006	20 March	15 May	56 Days	27 March	15 May	49 Days	27 March	22 May	56 Days
2007	15 March	15 May	61 Days	19 March	19 May	61 Days	26 March	26 May	61 Days
2008	24 March	24 May	61 Days	31 March	24 May	54 Days	31 March	24 May	54 Days

Year	Zone 1			Zone 2			Zone 3		
	Start	**End**	**Duration**	**Start**	**End**	**Duration**	**Start**	**End**	**Duration**
2009	16 March	9 May	54 Days	23 March	16 May	54 Days	30 March	23 May	54 Days
2010	8 March	17 April	41 Days	8 March	24 April	48 Days	15 March	9 May	56 Days
2011	21 March	13 May	54 Days	21 March	20 May	61 Days	28 March	27 May	61 Days
2012	5 March	27 April	54 Days	12 March	11 May	61 Days	19 March	11 May	54 Days
2013	11 March	10 May	61 Days	18 March	17 May	61 Days	25 March	31 May	68 Days
2014	31 March	23 May	54 Days	7 April	30 May	54 Days	7 April	30 May	54 Days
2015	30 March	22 May	54 Days	6 April	29 May	54 Days	6 April	5 June	61 Days
2016	14 March	13 May	61 Days	21 March	27 May	68 Days	28 March	3 June	68 Days
2017	27 February	05 May	68 Days	NA	NA	NA	NA	NA	NA

1. (NA) no data available.

3.4 **Road Roughness Measurement**

The idea of this research is to replace the use of FWD readings with measurements to be able to identify the period of time when the thawing reduces the bearing capacity of any pavement. The suggested approach is to by using an accelerometer to measure the pavement roughness given the low cost of such solution. In general vehicles respond to different road surface conditions, therefore, vehicles can be used with an accelerometer to estimate road surface condition. Accelerometers can be used to capture vertical accelerations which are correlated to road surface condition. Accelerometers can be found in most tablets and smartphones. By placing a smartphone that comes with acceleration sensors, the variation

of the vibration is to believe to be captured. Smartphone sensors capture accelerations in three-dimensional fashion. The vertical movement is only used in this thesis.

The variation in the acceleration-z data is utilized to derive the standard deviation of the vertical movement. Mean speed then normalized the standard deviation to provide indication for the road surface condition, RI. The results obtained reflect the condition for the pavement surface whether it is in a good condition or bad condition (**figure 3.3**).

3.4.1 A proxy of International Roughness Index

According to (Amador-Jiménez & Matout, 2014), the road roughness can be estimated using the following equation. The speed normalized the standard deviations of z_acceleration.

$$\frac{\sigma_z}{v_{yi}} = \frac{\sqrt{\frac{1}{n}\sum_{i=1}^{N}(a_{zi}-\bar{a})^2}}{v_{yi}} \qquad (5)$$

(σ_z) is the Standard deviation of z_acceleration and (v_{yi}) is the average vehicle speed. Values of the standard deviation over the average speed and multiplied by 100 can be used as proxy for RI.

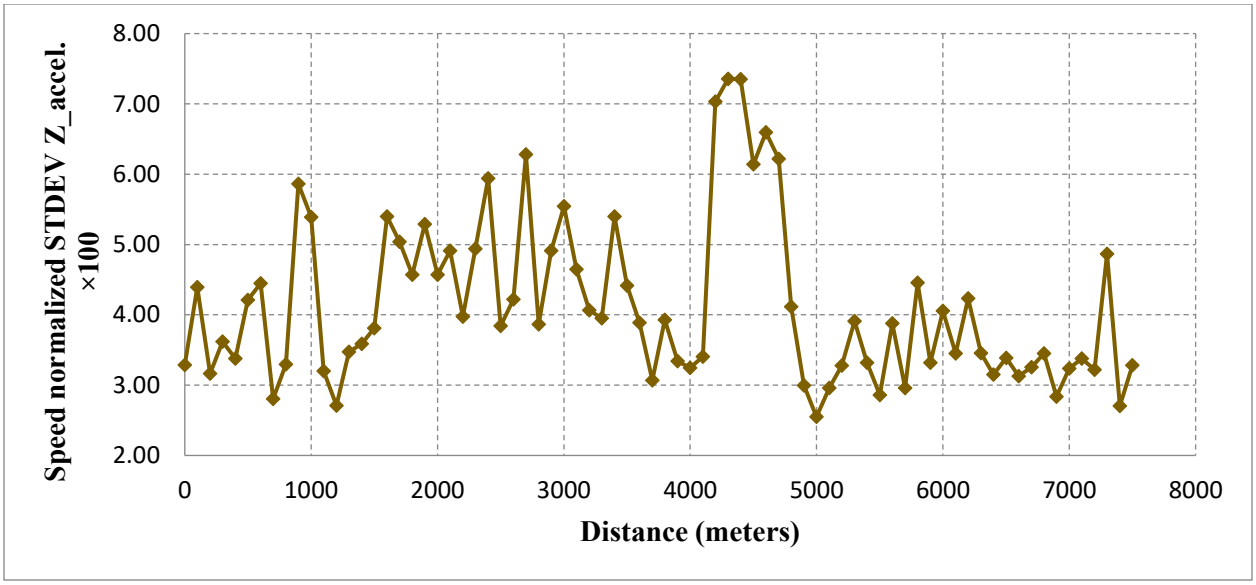

Figure 3-3 Pavement roughness for the tested segment, captured on September 28, 2016

3.4.2 Data Collection Procedures

Figure 3.4 summarizes the overall data collection and processing procedures. First, an application records vertical movement accelerations, speed, and time stamp. Then the collected data is brought altogether into a spread sheet. An Excel Macros is used to process the data to estimate one value per second. Such value reflects the speed normalized standard deviation of the z_acceleration multiplied by a factor of 100 as recommended by previous research.

Smartphones contain accelerometers to control their screens orientation. Thus, these devices are able to log accelerations. Also, the spatial coordinates (Latitude, Longitude) and speed could be recorded. During the data collection, the, smartphone orientation was fixed within the vehicle.

The mobile device was placed on a flat surface on the arm rest beside the driver every time while the data was logged. Proper fixture of the phone was inspected before running

the data collection to ensure the accuracy in recording data. **Table 3.3** below is a brief illustration of the equipment used in data collection processes.

Table 3-3 Equipment used to collect data required.

Mobile device type	Application	Vehicle
• (Smartphone) Samsung Galaxy S4/ 16 GB. • Android system.	○ AndroSensor application records**:** • Speed (m/s), (km/hr). • Accelerations (x, y, z). • Coordinates (longitude & latitude).	• KIA Forte 2011. • Full inspection was done before the data collection.

The pavement roughness data collection begins with a vehicle at a speed of 60 to 80 (km/hr) and ends at the same speed. One person (the driver) is in the car and its weight becomes part of the overall load. The vehicle was driven on the right lane for the entire segment as it is considered the most deteriorated lane in any road section. Data were captured at intervals of 0.100 of a second. The Samsung Galaxy S4 laid in a horizontal position on a flat surface as previously explained. The screen of the smartphone was facing up and the head was pointing toward the front of the vehicle. Thus, the accelerations (x, y, z) represent the motion among left-right, front-back, and up-down, respectively. In this research just the z-acceleration was retained. It represented the vertical movement of the vehicle which reflected the pavement roughness condition.

From a practical perspective two data procedures protocols were required: The Site Work and the Computer Work. The following the steps are sorted by order.

Site Work:

1. Set the mobile device in the vehicle on a flat surface while fully attached.

2. Verify the intervals of data collection.

2. Start recording data at speed of 70 km/hr.

3. Drive the vehicle non-stopping and maintain constant speed.

4. Stay on the right lane for the entire segment as possible.

5. Stop recording data when reaching the end of the proposed segment.

6. Export the collected data from the mobile device to the computer (using email or any other suitable mean) to the purpose of Computer Work.

Computer Work:

This stage is essential to process data obtained from the site work stage. Its importance's comes from the side that the standard deviation of the z-acceleration and mean speed could be obtained and reflects the pavement condition. The computer work steps are:

1. Join the accelerations, coordinates and speed data in Excel sheet.

2. Calculate the standard deviations of the z-accelerations per second (using 10 points per second).

3. Estimate the mean speeds every second in meter per second (10 captured data).

4. Normalize the standard deviation of z-acceleration by dividing it by the corresponding mean speed for each second.

5. Multiply each normalized standard deviation by 100 to obtain the Roughness Index RI.

6. Generate a column for the coordinates (latitude & longitude) for each second.

7. Use Excel Macro to remove blank spaces.

8. Export organized data in CSV format to ArcMap.

9. Join data progressively through time to reflect measured RI values every week.

10. Draw a comparison graph of RI versus cumulative distance for each week of data collection.

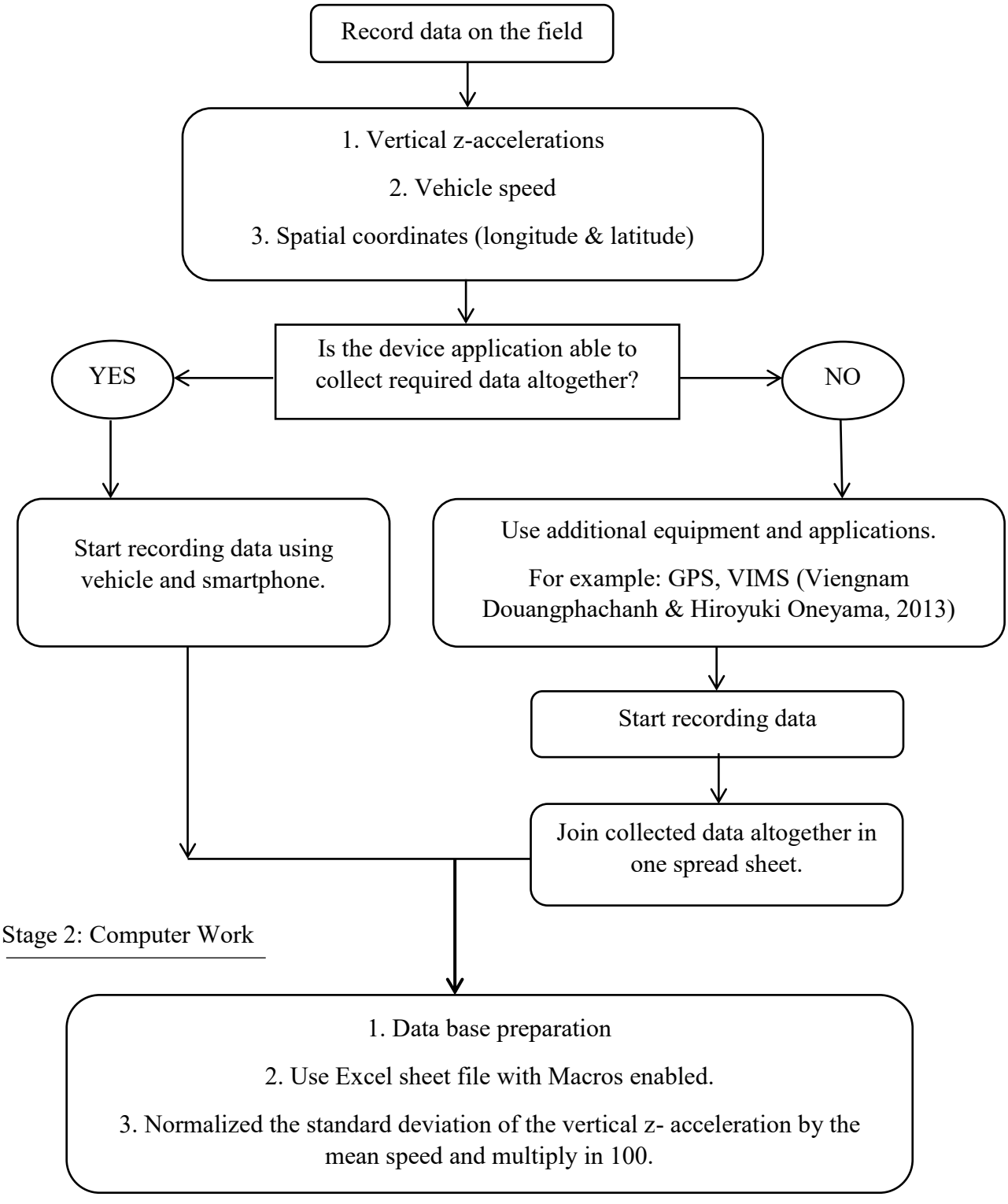

Figure 3-4 Data collection & processing flow chart

Figure 3.5 shows a sample of data captured on the week 30th, on May 17, 2017 at 11:38 pm. The figure shows the data including spatial coordinates (longitude & latitude), as well as the RI calculation per second. It is clear from the figure that 10 blank spaces are generated in between each estimate of roughness along with its coordinates and time stamp.

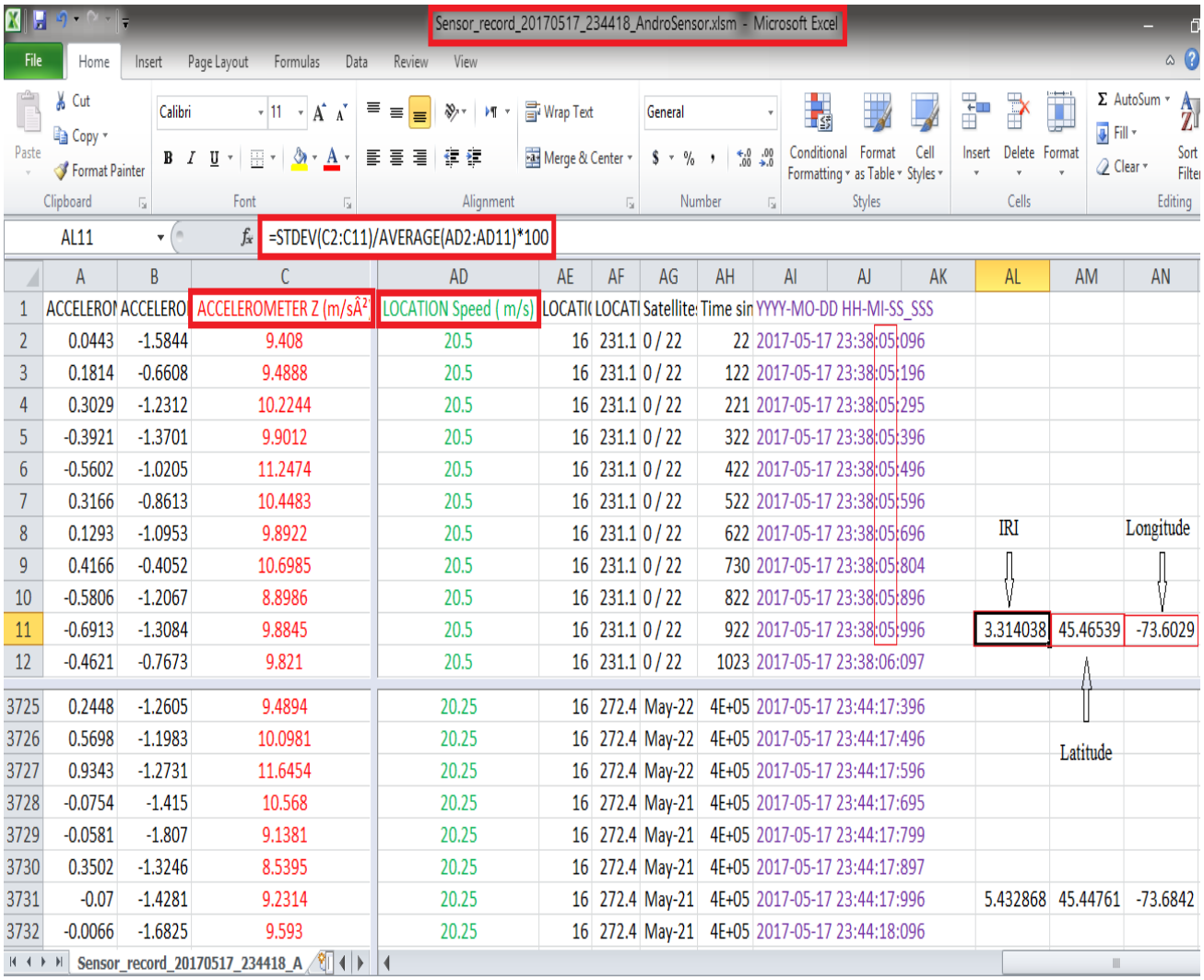

Figure 3-5 Screenshot of Excel Spread Sheet with RI calculation.

If the mobile device is unable to record data altogether, thin as suggested in the flow chart; Global Positioning System (GPS) and Vehicle Intelligent Monitoring System (VIMS)

(Douangphachanh & Oneyama, 2013) may could use. However, in this research the Samsung Galaxy S4 was able to collect vertical accelerations, vehicle velocity, and coordinates data altogether; there was no need to use the GPS and VIMS.

3.4.3 Data Processing

Missing coordinates were found on data during December. Such coordinates were imputed in the data by interpolating between known data points with coordinates. For this purpose and as seen on **figure 3.6**, Excel was used to equally distribute changes in latitude and longitude.

For the calculations to be successful, certain mandatory reorganizing data were utilized. New columns were generated; Lat_f, Long_f, Count_lat, Count_long, Delta_lat, Delta_long, and ratio. Each column represents a certain equation except ratio column. The desire of creating these columns is to adjust the road profile section lay out in a way that simulate the real profile and increase the precision in the RI values.

The Latitude_final and Longitude_final columns represent reliable and final spatial coordinates. These two columns were established based on count_latitude, count_longitude, delta_latitude, delta_longitude, and ratio. The count_lat and count_long detect the changes in latitude and longitude values that were captured by smartphone device. Also, they divide the subsections into certain points to give each point consistent coordinates. The delta_lat and delta_long are the distance between two respective coordinates. The distance remains constant till latitude or longitude change. Lastly, ratio column has different values; each value is the total points between the two following coordinates in the subsections. Ratio column uses to divide count_lat and count_long to enhance in final coordinates calculations.

Few calculations are needed in each previous column to approach the reliable spatial coordinates. The following formula was used in excel sheet file to create the Lat_f for each point (each raw). The same formula is also utilized to establish the Long_f.

$$\text{lat\_f} = \text{Prevoius Latitude} + \left(\text{delta\_lat} \times \frac{\text{count\_lat}}{\text{ratio}}\right)$$

Figure 3.6 shows the pavement roughness data collected on December 6, 2016 and the implementation of the coordinate's imputation in Excel. The Latitude and Longitude values have not been changed from the serial number 2 till 17; on the other hand, the Lat_f and Long_f have different values comparing to previous values in each serial point. The RI values remain the same with no changes in calculations.

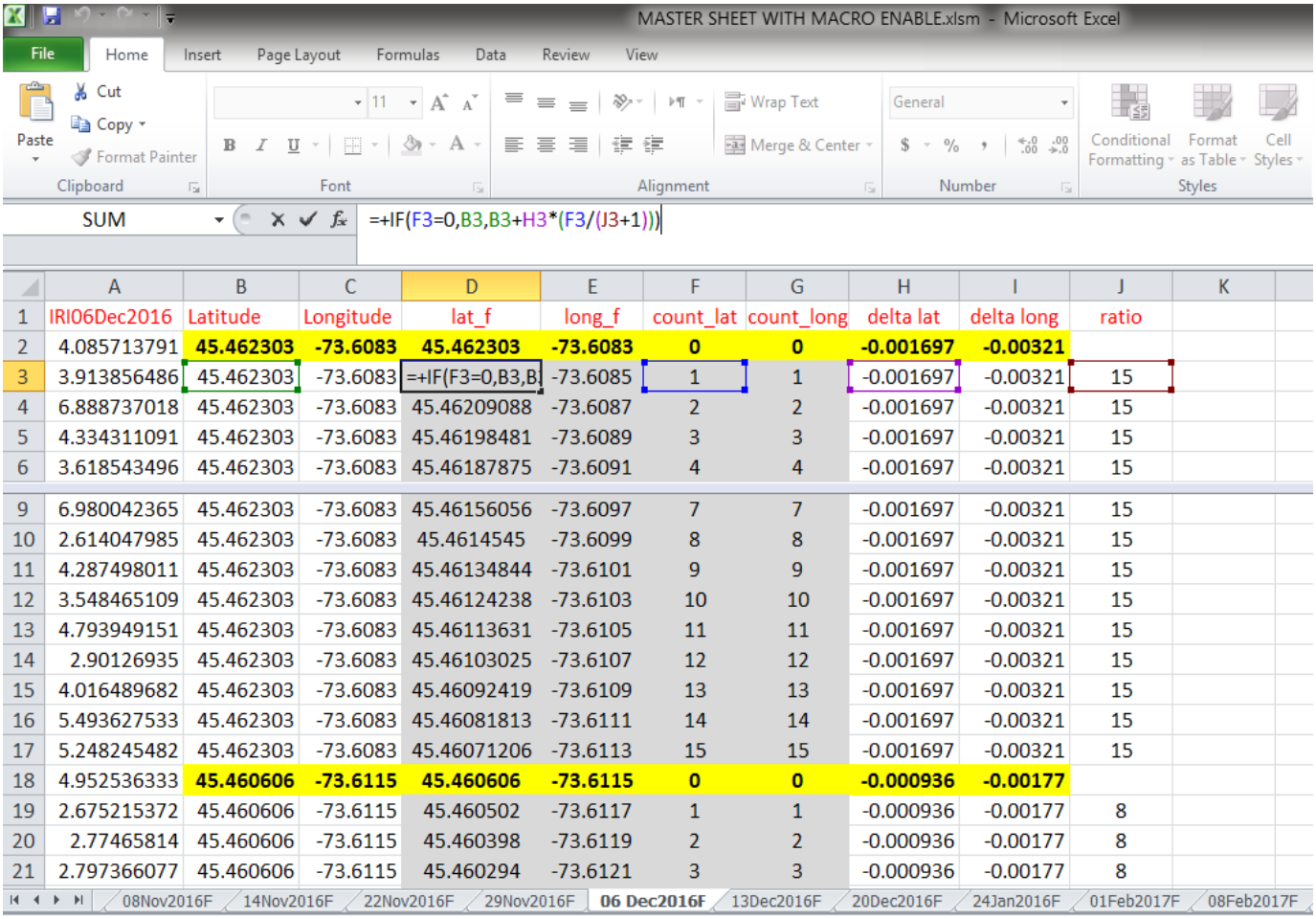

	A	B	C	D	E	F	G	H	I	J	K
1	IRI06Dec2016	Latitude	Longitude	lat_f	long_f	count_lat	count_long	delta lat	delta long	ratio	
2	4.085713791	**45.462303**	**-73.6083**	**45.462303**	**-73.6083**	**0**	**0**	**-0.001697**	**-0.00321**		
3	3.913856486	45.462303	-73.6083	=+IF(F3=0,B3,B	-73.6085	1	1	-0.001697	-0.00321	15	
4	6.888737018	45.462303	-73.6083	45.46209088	-73.6087	2	2	-0.001697	-0.00321	15	
5	4.334311091	45.462303	-73.6083	45.46198481	-73.6089	3	3	-0.001697	-0.00321	15	
6	3.618543496	45.462303	-73.6083	45.46187875	-73.6091	4	4	-0.001697	-0.00321	15	
9	6.980042365	45.462303	-73.6083	45.46156056	-73.6097	7	7	-0.001697	-0.00321	15	
10	2.614047985	45.462303	-73.6083	45.4614545	-73.6099	8	8	-0.001697	-0.00321	15	
11	4.287498011	45.462303	-73.6083	45.46134844	-73.6101	9	9	-0.001697	-0.00321	15	
12	3.548465109	45.462303	-73.6083	45.46124238	-73.6103	10	10	-0.001697	-0.00321	15	
13	4.793949151	45.462303	-73.6083	45.46113631	-73.6105	11	11	-0.001697	-0.00321	15	
14	2.90126935	45.462303	-73.6083	45.46103025	-73.6107	12	12	-0.001697	-0.00321	15	
15	4.016489682	45.462303	-73.6083	45.46092419	-73.6109	13	13	-0.001697	-0.00321	15	
16	5.493627533	45.462303	-73.6083	45.46081813	-73.6111	14	14	-0.001697	-0.00321	15	
17	5.248245482	45.462303	-73.6083	45.46071206	-73.6113	15	15	-0.001697	-0.00321	15	
18	4.952536333	**45.460606**	**-73.6115**	**45.460606**	**-73.6115**	**0**	**0**	**-0.000936**	**-0.00177**		
19	2.675215372	45.460606	-73.6115	45.460502	-73.6117	1	1	-0.000936	-0.00177	8	
20	2.77465814	45.460606	-73.6115	45.460398	-73.6119	2	2	-0.000936	-0.00177	8	
21	2.797366077	45.460606	-73.6115	45.460294	-73.6121	3	3	-0.000936	-0.00177	8	

Figure 3-6 Excel Spread Sheet with Macro enabled to calculate corrected Latitude (Lat_f) and Longitude Long_f

3.5 Geographic Database Preparation

Data collected from the site was plot over the map to better understand the effect of freeze thaw cycles on the pavement roughness. For this reason data collection proceed on a periodical basis, and each new data was added to the Geographic Information System (ArcGIS). Data transferred to ArcMap was used to obtain the average condition for the road segment used in this research. The following steps and frame work (**figure 3.8**) illustrate the data preparation processes corresponding with the study case:

1. Gathered data in a comma separated vector (csv) format was imported into ArcMAP

2. Each week of data was added to the previous dataset into ArcMAP.

3. Coordinated were projected following WGS-1984 geographic system **(figure 3.7).**

4. Average RI was calculated for subsegments of 100 meters.

5. Files are progressively saved as a new shape file in ArcMap.

6. All attribute data are exported back to Excel sheet and a profile of roughness per meter is compared across various dates of data collection.

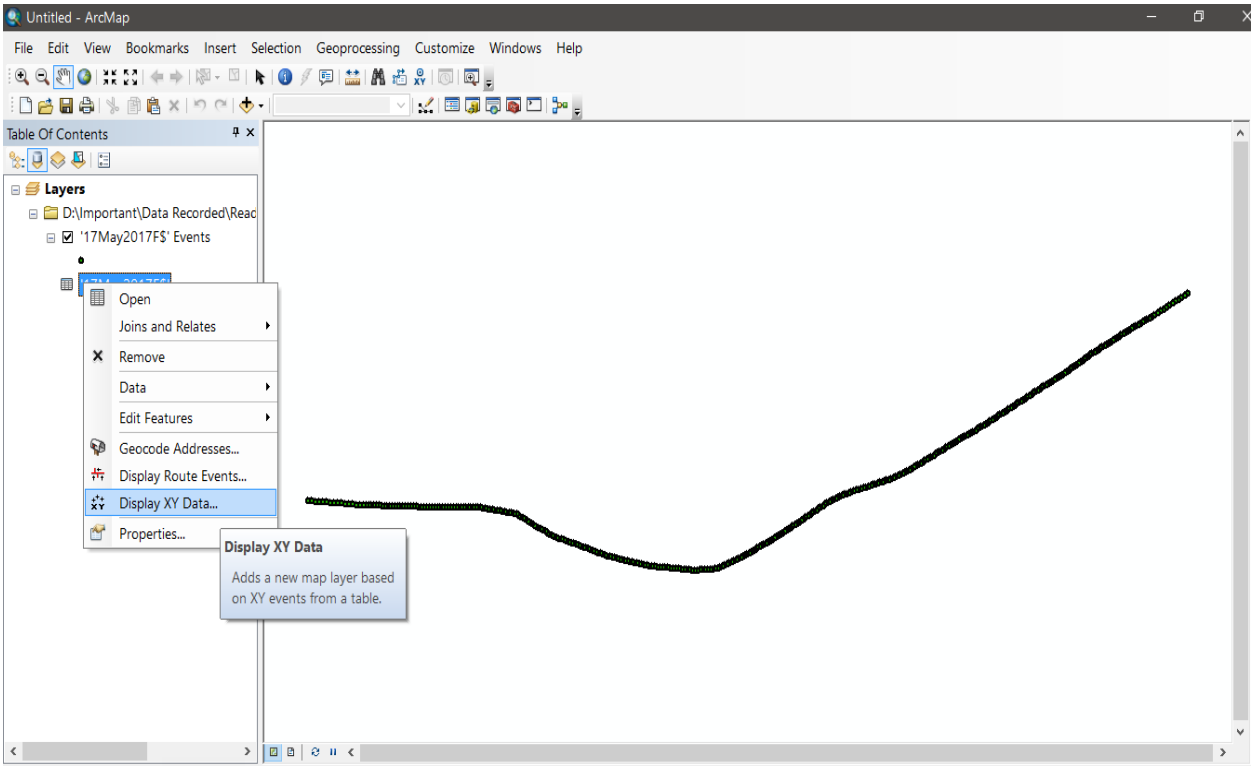

Figure 3-7 Point-feature data over road test-section showing by ArcMap

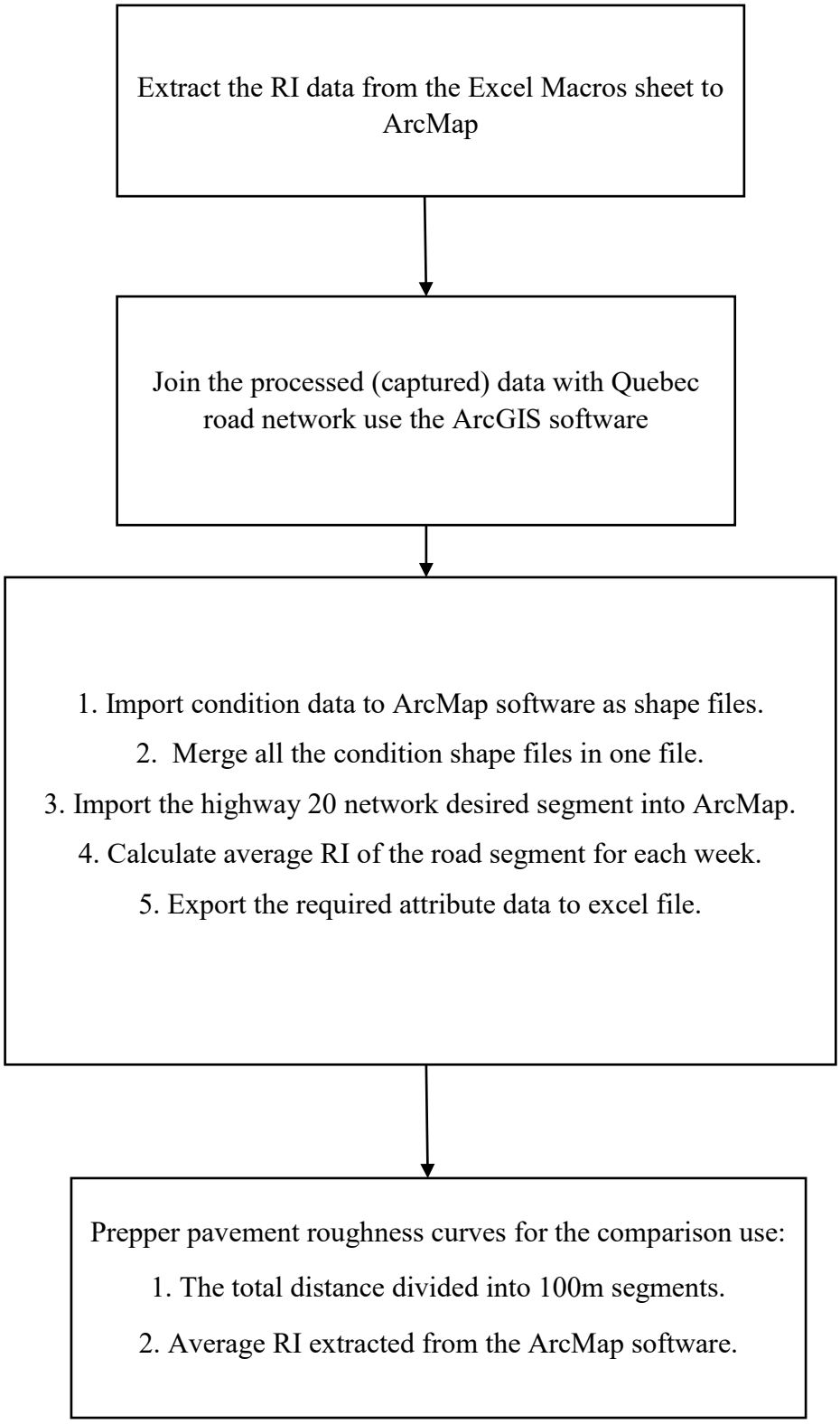

Figure 3-8 Data base preparation framework using ArcGIS platform

CHAPTER 4

4 Data Analysis and Results

4.1 Introduction

This chapter demonstrates pavement surface roughness variations through different three periods. Few charts that reflect pavement surface condition were created in order to compare the RI for different seasons to detect the overall changes in the pavement roughness RI. After eight months of recording, the desired pavement was deteriorated with an increase in the RI value during the thawing season and drastically changes were found. The average RI was raised from 3.99m/km in fall to 5.30m/km in spring. In accordance, RI in different cities in Canada were estimated by AASHTO equation.

4.2 Data Analysis

Data were recorded on the desired section for more than 8 months, once a week for 30 weeks to monitor changes on pavement roughness. During that period, the pavement surface experienced significant changes that affected the pavement smoothness. These changes resulted from various aspects such as temperature variations, soil moisture, pavement materials, and traffic flow.

Results obtained were capable of identifying the road surface condition. The following figures show the pavement surface in three different seasons (fall, winter, and spring), neglecting the summer season as it is not considered in the freeze-thaw period. The data were captured on September 28, 2016, February 01, 2017, and May 17, 2017, respectively. The higher the RI is, the more the pavement deteriorated. For comparison facility, and for the

following figures, each chart line color has been fixed to the season that data was recorded in: The brown color for the fall season, the blue color for the winter season, and the red color for the spring season.

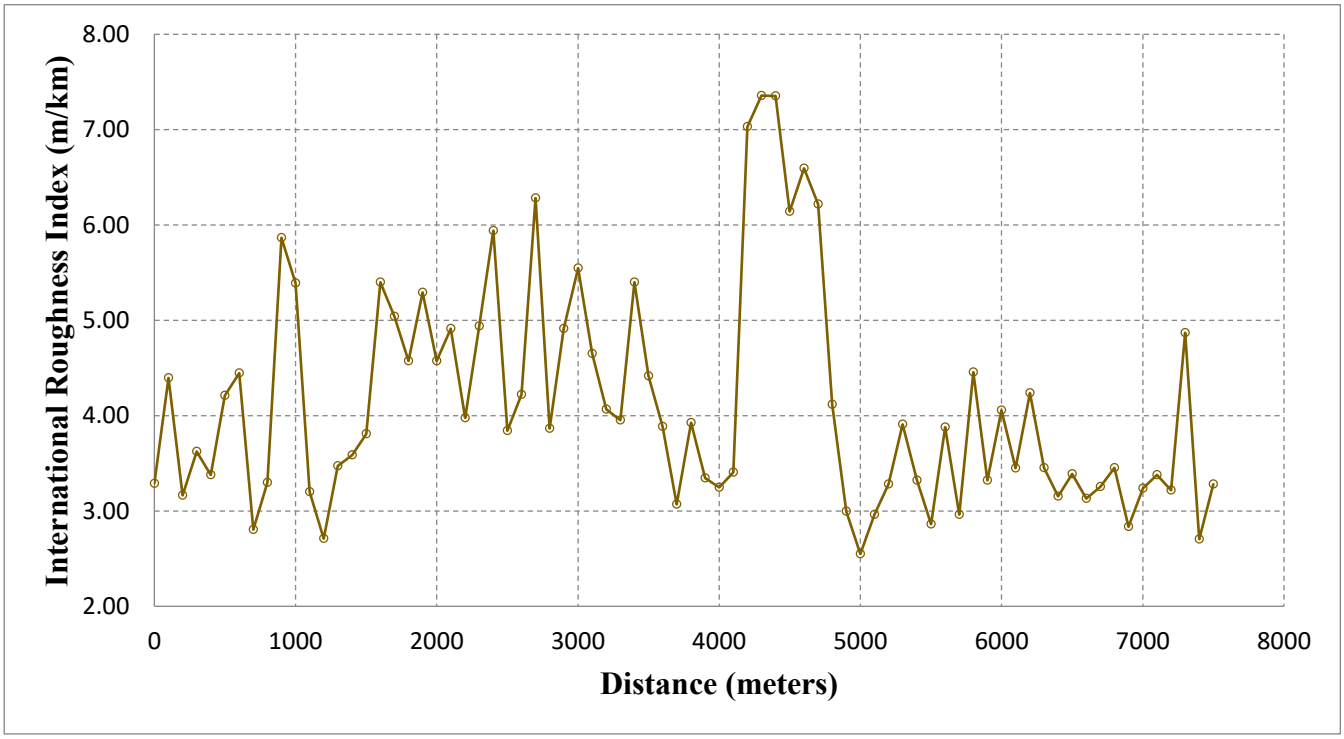

Figure 4-1 Estimated pavement-surface roughness on September 28, 2016.

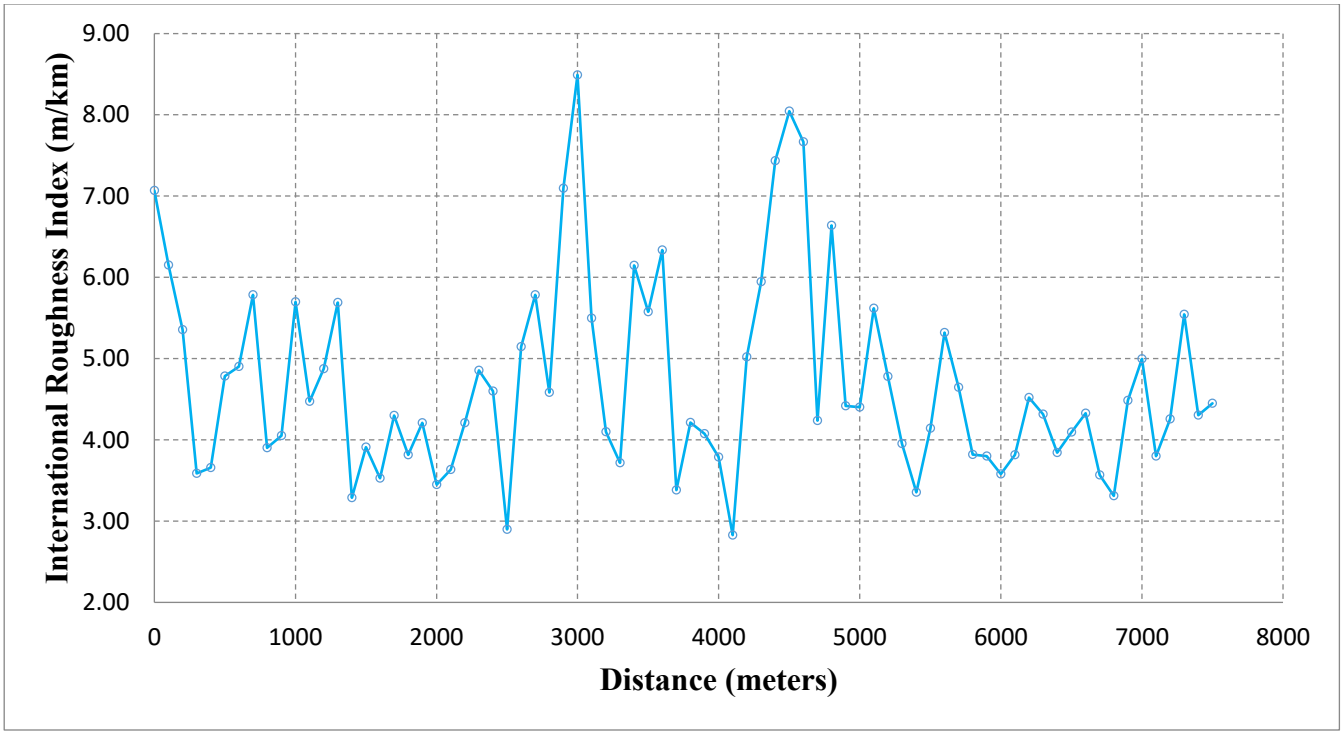

Figure 4-2 Estimated pavement surface roughness on February 01, 2017

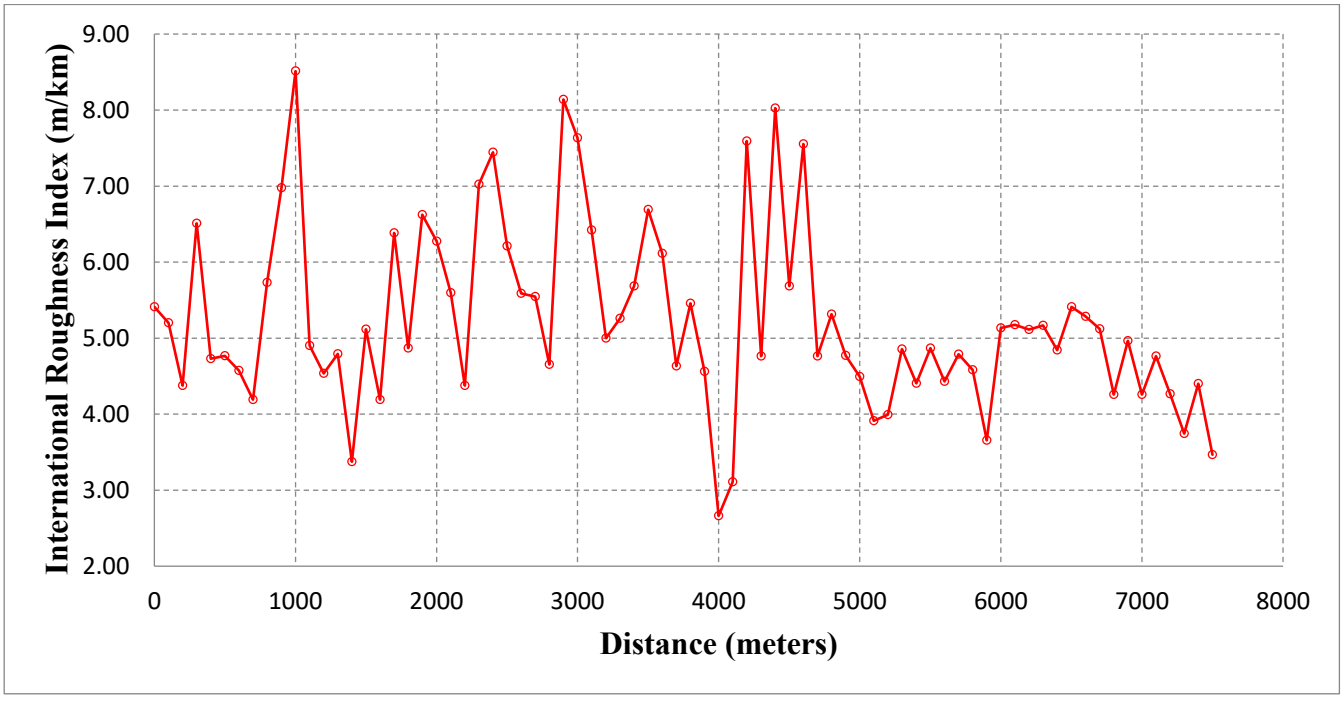

Figure 4-3 Estimated pavement surface roughness on May 17, 2017

4.3 Air temperature Variations

Variations in the air temperature serve as indirect indicator of freeze-thaw cycles observed in one day. After comparison the air temperature before, during, and after the spring thaw period, three days were selected as an excellent case to present the freeze-thaw cycle effect and to show the variations in the pavement surface condition.

Table 4-1 Selected air temperature records, Montreal, Quebec (Canada Government, 2017).

week	Day	Month	Year	Max temp (℃)	Min temp (℃)
1	28	9	2016	21	10.1
2	4	10	2016	19.3	5.1
3	11	10	2016	16.7	3.1
4	18	10	2016	24.3	8.4
5	25	10	2016	6.9	-0.6
6	1	11	2016	11.2	-0.3
7	8	11	2016	16	0.8
8	14	11	2016	13.1	4.7
9	22	11	2016	-0.1	-1.8
10	29	11	2016	2.2	-1.6
11	6	12	2016	1.3	-7
12	13	12	2016	2.2	-7.5
13	20	12	2016	-0.1	-17.1
14	24	1	2017	-2.3	-3.8
15	1	2	2017	-6.3	-13.9
16	8	2	2017	3.9	-9.8
17	14	2	2017	-3.5	-11.9
18	21	2	2017	3.3	-8.2
19	28	2	2017	8.3	-4.6
20	7	3	2017	6	-2.9
21	16	3	2017	-3.4	-9.9
22	21	3	2017	3.6	-3
23	28	3	2017	4.8	0.8
24	4	4	2017	5.6	2.1
25	11	4	2017	14.1	4.7
26	18	4	2017	9.5	0.6
27	25	4	2017	15.2	1.8
28	2	5	2017	16.4	7.5
29	9	5	2017	8.8	0.6
30	17	5	2017	29.3	14.1

Table 4.1 shows air temperature for the city of Montreal, Quebec, during the same days of the data collection campaign. For the duration of December 21, 2016 to January 23, 2017 no data were recorded, that period considered as a part of the frozen cycle. However, other data were captured through the frozen period for comparison purpose.

4.4 Comparison of Same Pavement Surface for Different Seasons

The test was done to compare the pavement surface fluctuation before and after one environmental cycle containing various frost heave days. After analyzing all the data, it has been found that the most representative data for the fall, winter, and spring seasons was captured on September 28, 2016, February 01, 2017, and May 17, 2017. Therefore, these three days were combined altogether in one figure to show the differences in the pavement surface on three specific points on time. **Figure 4.4** compares of the International roughness index for the same pavement surface in different seasons (fall, winter, and spring). The summer season was not considered as the frost and heave occurs at the end of winter and beginning of spring seasons. However, summer season could be considered for more relevant evidence in future experiments.

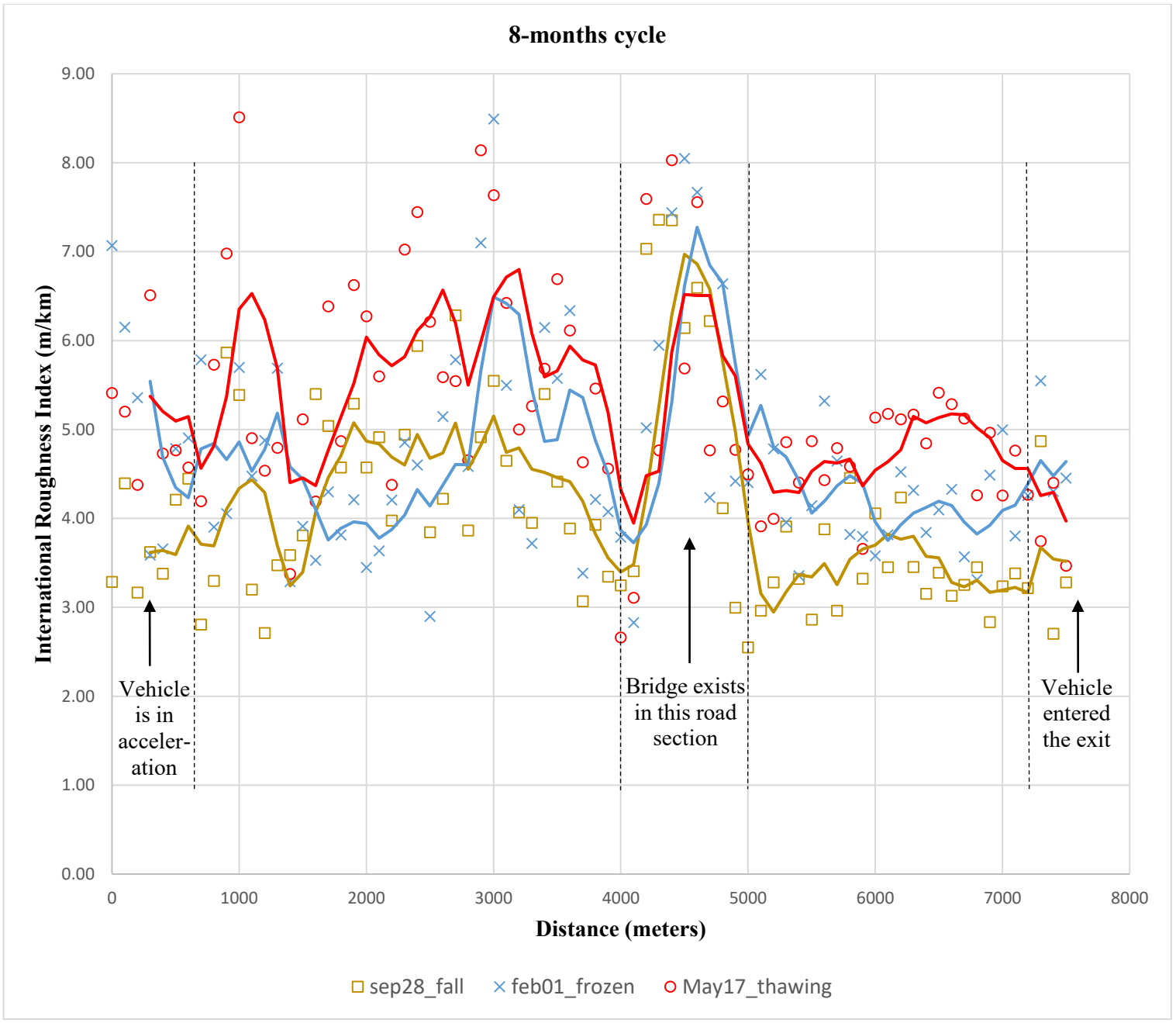

Figure 4-4 Comparison of pavement-surface roughness for the sample site in different seasons.

It is clear that the freeze-thaw cycle impacted the subgrade soil layer which translated into the pavement surface as it has been shown in **figure 4.4.** The average RI value before the frost season was found to be 3.99 m/km, while during winter season was 4.52 m/km, and in spring season was 5.30 m/km.

As a result of frost penetration in all pavement layers and the crystallization of ice within the larger soil voids, soil particular volume increased and reflected on the pavement surface layer as cracks and distortions. However, pavement surface roughness may improve and reduction in the RI values may occur due to soil volume expansions. The previous **figure 4.4** showed that the RI values were decreased in the road section between 1600m to 2800m. In some cases, soil particular expands under deflected layers, which pushes these layers upward the surface. This condition adjusts pavement anomalies and bumps into a smooth pavement surface and decrease pavement distortions.

Finally, in the heave period, the RI significantly increased and the pavement surface became rougher than in winter. The average RI values were higher than other seasons with maximum of 6.8 m/km and minimum of 4.3 m/km. The topping layer experienced excessive fatigue damage owing to loss of support of the underneath layers. That is due to ice melt down in the subgrade soil layer as well as high moisture content which makes the surface layer very loose and soft.

However, few discrepancies were found in the chart as of the begging of the test and at the end. From distance 0 to 1000 meters the vehicle velocity is not constants but rather accelerating and still not tracked on the right lane. While at the end of the test after 7000 meters, the driver was recording data even after proceeding through the exit 60. That action led to some inaccurate collected point data at the begging and at the end of the test. Thus,

those points were removed. Also, the road section between the milepost 4000 to 5000 meters showed very close RI values, this is possible a result of a bridge located at that section. The subgrade soil layer does not exist and the frost heave phenomenon is not applicable.

Figure 4.5 shows the RI values for the same pavement surface for different seasons. However, the RI values for the distance between 4000m and 5000m in **figure 4.4** were discarded, hence the bridge section was removed from the chart to show a clear indication of the RI value changes as well as the freeze-thaw impacts on the subgrade soil layer (**figure 4.5)**. In addition, **figure 4.6** shows the average RI for the same pavement surface after removing the first section of the road segment where vehicle was in acceleration, as well as last section where vehicle procced through the exit.

Even after removing the initial middle and final sections, it is difficult to observe a constant trend of RI differences, suggesting that closer dates with RI values will not be able to capture RI changes and to identify the beginning and the ending of the load restriction season for trucking. Henceforth, the first part of the objective of this research cannot be satisfied with weekly (or shorter timed) measurements of RI.

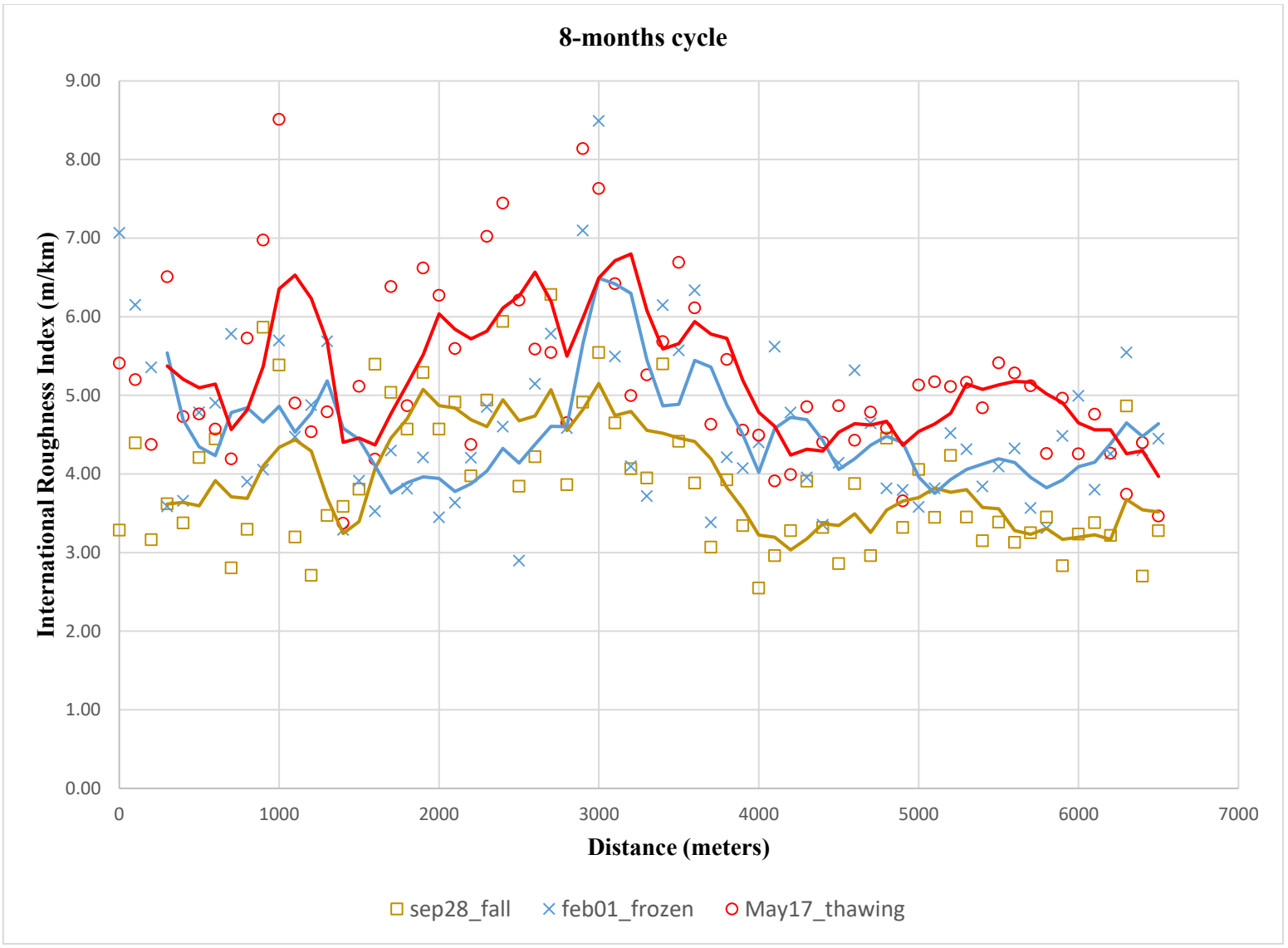

Figure 4-5 Comparison of the pavement-surface roughness after removal of bridge section

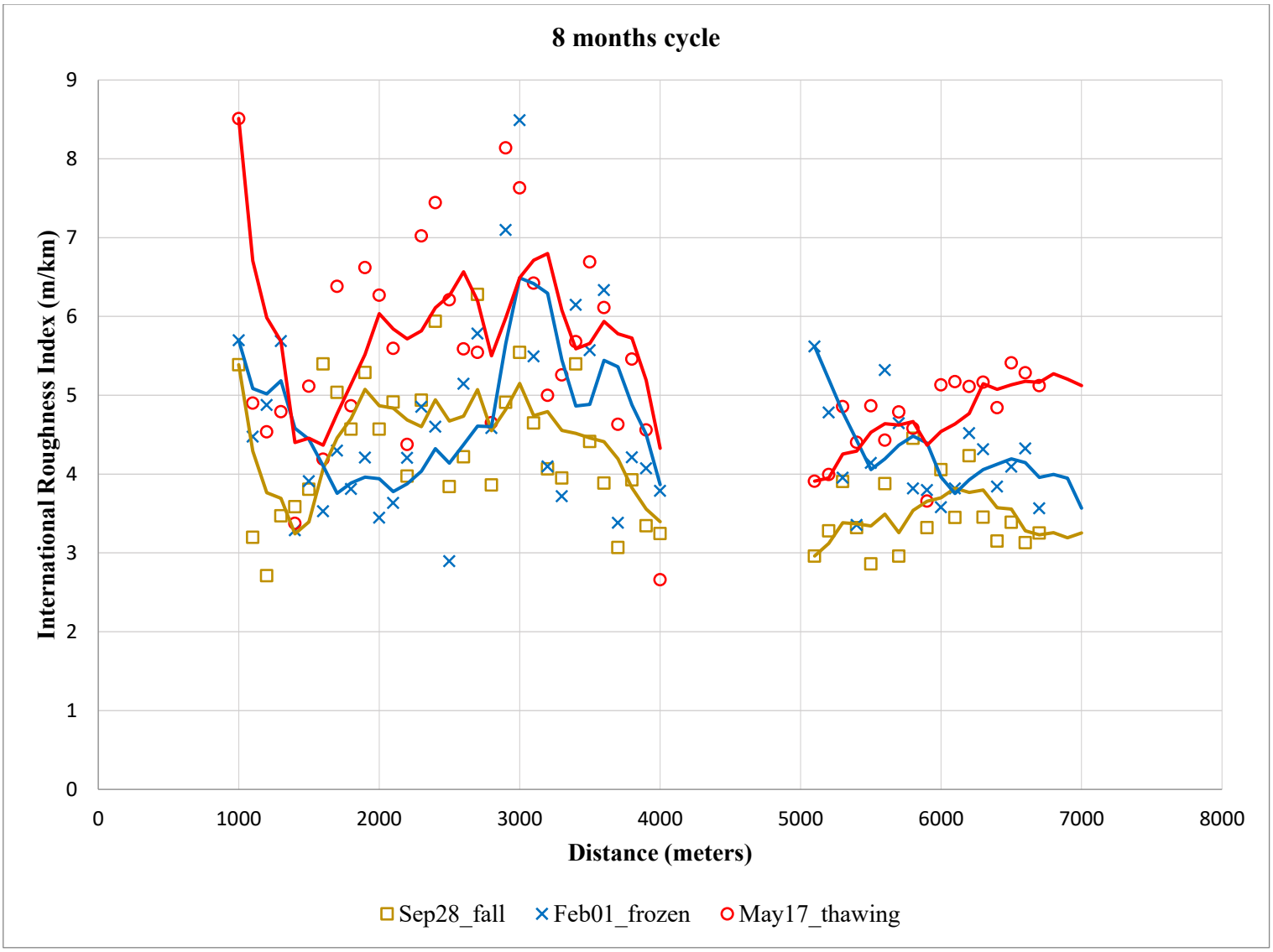

Figure 4-6 Clean Comparison of Pavement-surface roughness after removal of start/end and bridge sections.

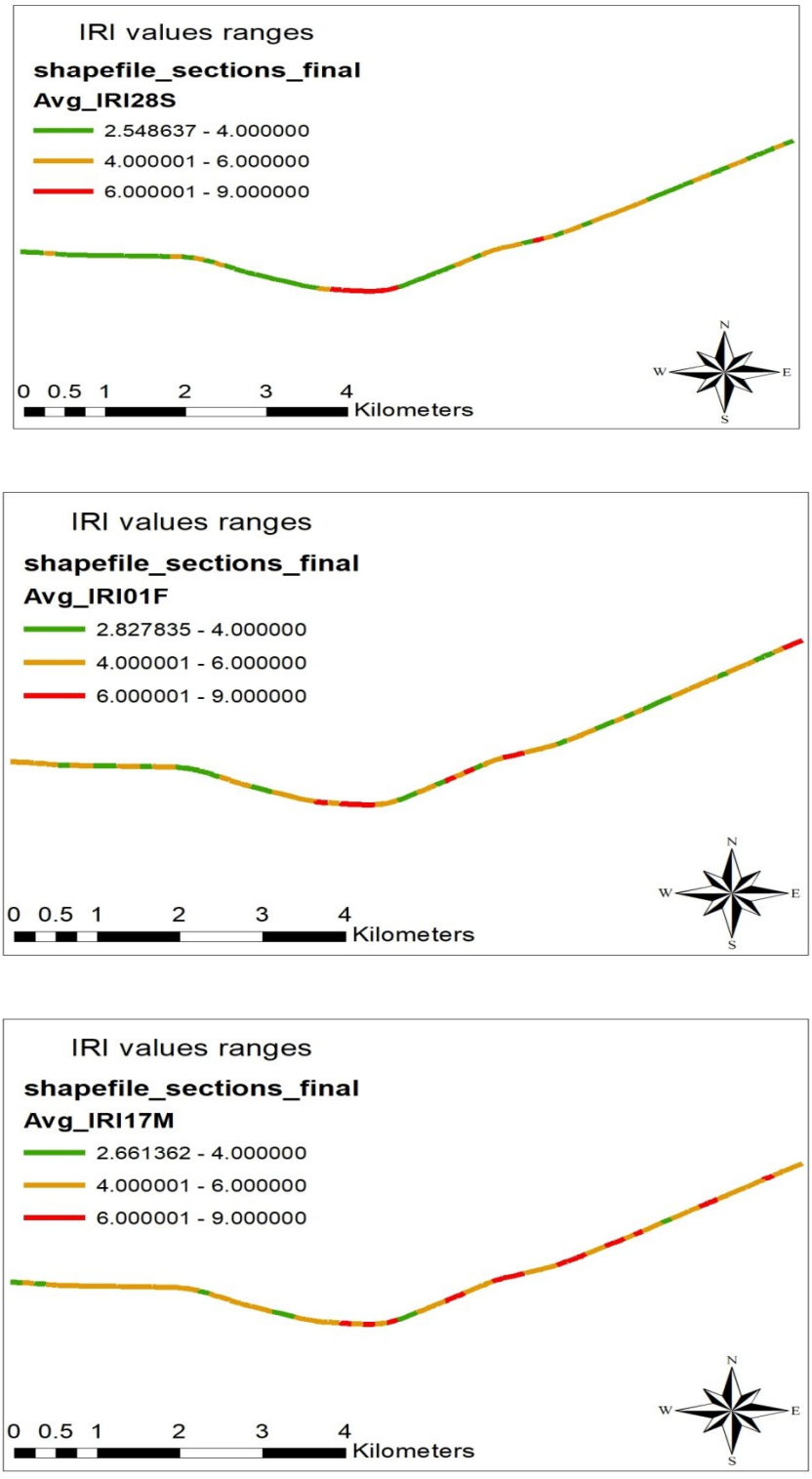

Figure 4-7 Pavement-surface roughness time-progression

Table 4-2 Color-coded Pavement-surface roughness

Color	Range of RI values
Green	4 or below
Orange	4.1 – 6
Red	6.1 or more

Figure 4.7 shows the test-section for three different seasons. The observed deterioration can be appreciated on the map according to the color codes of table 4.2.

4.5 The RI Estimation for Different Cities in Canada

Having estimated the variation in RI for the sample segment of highway 20 in Montreal, AASHTO (Guide for Mechanistic-Empirical Design) method could be used to estimate the expected impact of freeze-thaw cycles and moisture supply at other Canada cities.

First, the expected age is estimated and fixed, and then RI changes after one year are estimated for various cities. The RI was calculated and influenced by different climatic regions in Canada. The utilized equation is (AASHTO, 2001) :

$$RI = RI_o + 0.0463 \left[\frac{\ln(FI+1)\,(P_{0.02}+1)(\ln(Rm+1)}{10}\right]\left(e^{\left(\frac{age}{20}\right)}-1\right) \qquad (6)$$

RI: the International Roughness Index after thawing.

RI_o: the initial International Roughness Index (before the frozen season).

FI: average annual freezing index (given by the summation of the degree-days for a freezing season with daily mean temperature below zero).

$P_{0.02}$: Subgrade % of 0.02 mm = 30%

Rm: mean annual rainfall.

Age: age of the section.

4.5.1 Pavement Age Period

Pavement age is playing a significant role in the pavement design factors. Pavement period was computed from the previous equation. In this research, the equation was first applied on the city of Montreal as the average RI from **figure 4.6** changed on average from 3.99 to 5.30 m/km. However, the freezing index was extracted from a research done by Malcolm and Thomas with freezing index for the provinces of Canada in units of (degree-days °F).

Table 4-3 Freezing index for Canadian provinces (Malcolm D Armstrong & Thomas I Csathy, 1963).

Provinces	Freezing Index (Degree-days °C)
Britch Columbia	0 – 277
Alberta	1111 ─ 2222
Saskatchewan	1388 ─ 2500
Manitoba	1666 ─ 3333
Ontario north	833 ─ 2500
Ontario south	277 ─ 833
Quebec	1111 ─ 2222
Newfoundland	277 ─ 833
New Brunswick	833 ─ 1111
Pr. Edward Island	555 ─ 833
Nova Scotia	277 ─ 555

Additionally, the rain amounts were given by environment Canada. The annual average rain precipitation of the year 2017 was selected for the cities indicated below.

Table 4-4 Annual-average rain-precipitation in major cities in Canada (Statistics Canada, 2017)

City	Annual Average precipitation (mm)
Halifax	1452.2
Montreal	978.9
Toronto	792.7
Winnipeg	513.7
Regina	388.1
Calgary	412.6
Vancouver	1199

Also, the percentage of the soil with 0.02mm in the subgrade layer was assumed to be 30%, given the lack of site measurements. The FI used in the following calculations, corresponds to the mean values from **table 4.3** for each province.

4.5.1.1 Pavement Age Calculation

$$5.30 = 3.99 + \left[0.0463 \times \frac{\ln 1667 \times 1.3 \times \ln 979.9}{10}\right] \times \left(e^{\left(\frac{age}{20}\right)} - 1\right) \qquad (6)$$

$$5.30 = 3.99 + 0.307\left(e^{\left(\frac{age}{20}\right)} - 1\right)$$

$$1.617 = 0.307 \times e^{\left(\frac{age}{20}\right)}$$

$$\ln e^{\left(\frac{age}{20}\right)} = \ln 5.259$$

$$age = 33.20 \approx 33 \text{ years}$$

Pavement age and initial pavement condition were fixed for the following calculations in order to compare the amount of expected deterioration from one environmental cycle at different places in Canada.

4.5.2 RI deterioration from one environmental cycle for different cities

Pavement-surface roughness (RI) values were calculated using **equation 6** for various cities in order to acquire a sense of the extent of damage progression after one cycle. This includes truck traffic and environmental aspects combined, but serves as an indication of the rate of deterioration at different Canadian climates. A sample calculation is presented for the city of Vancouver below. The other RI values are reported in **table 4.5**.

Sample Calculation for the city of Vancouver:

$RI_o = 3.99$

Pavement age = 33 years

FI = 138 degree-days ℃

Rm = 1199 mm

$P_{0.02} = 30\%$

$$RI = 3.99 + \left[0.0463 \times \frac{\ln(138+1) \times (1+0.30) \times \ln(1199+1)}{10}\right] \times \left(e^{\left(\frac{33}{20}\right)} - 1\right) \quad (6)$$

∴ RI at the city of Vancouver = 4.875 m/km

Table 4-5 Values of pavement roughness design factors as well as the final RI for different cities

City	RI_o (m/km)	FI (degree-days ℃)	Rm (mm)	Pavement age (years)	Estimated RI (m/km) Total	Δ RI (m/km)
Halifax	3.99	416	1452.3	33	**5.102**	**1.112**
Montreal	3.99	1666	978.9	33	**5.284**	**1.294**
Toronto	3.99	555	792.7	33	**5.058**	**1.068**
Winnipeg	3.99	2500	513.7	33	**5.227**	**1.237**
Regina	3.99	1944	388.1	33	**5.133**	**1.143**
Calgary	3.99	1666	412.6	33	**5.121**	**1.131**
Vancouver	3.99	138	1199	33	**4.875**	**0.885**

5 Conclusions and Recommendations

5.1 Conclusion

Municipal governments assign considerable budgets to road assets mainly for the maintenance and rehabilitation of existing pavements. The freeze-thaw daily-cycles from each annual environmental cycle play a significant role in road deterioration and failure. Thus, detecting the initiation and end of such period is crucial for imposing load reductions on trucks. Traditional tools that have been used for this purpose are expensive and not all governments can afford. However, the low cost method proposed in this research could serve to record pavement roughness (RI) and its variations could be used to identify the beginning and the end of the freeze thaw cycles.

An experiment was carried out to obtain the International Roughness Index (RI) on highway 20 near Montreal. The method is very easy to operate and can be implemented frequently. A smart phone was backed on a vehicle to catch the variation on the vertical acceleration. The velocity normalized the vertical movement to approach the changes in the pavement roughness.

The data were recorded during 30 weeks, once a week. It was however difficult to perceive significant changes between any two weeks in order to monitor the decay in pavement condition and obtain an indication of the beginning of the load imposition. This was due in part because of the inability of the driver to repeat the exact same wheel path on each data measurement.

Three points on time (Fall, Winter, and Spring) were then selected to present the effect of the freeze-thaw cycles. From the analysis, it was possible to observe overall changes in

RI from fall to winter to spring, with average values reflecting a nearly 1.2 m/km change. These changes were then reflected via the mechanistic empirical pavement design guide equation into other locations in Canada, and it was found that significant changes in RI could be expected as well from one environmental cycle.

5.2 Recommendations

Self-driving vehicles could facilitate the collection of RI data through a cooperative environment in which each vehicle reports measured acceleration to a central repository of data, and hence a complete depiction of the roughness condition could be estimated. For future estimations one could increase the frequency of data collection to increase the accuracy of the data.

References

AASHTO. (2001). Guide for Mechanistic-EmpRIcal Design of New and Rhabilitated Pavement Structure. *National Cooperative Highway Research Program, Transportation Research Board, National Research Council*, 1-79.

Aho, A., & Saarenketo, T. (2006). Design and repair of roads suffering spring thaw weakening. *The ROADEX III Project, Northern Periphery*.

Amador-Jiménez, L., & Matout, N. (2014). *A low cost solution to assess road's roughness surface condition for pavement management.* Paper presented at the Transportation Research Board 93rd Annual Meeting.

Antunes, M., Litzka, J., Leben, B., La Torre, F., Weninger-Vycudil, A., Kokot, D., and Viner, H. (2008). The way forward for pavement performance indicators across Europe COST Action 354 Performance Indicators for Road Pavements Final Report.

Armstrong, D., & Csathy, T. (1963). Frost Design Practice in Canada-And Discussion. *Highway Research Record*(33).

Asefzadeh, A., Hashemian, L., Haghi, T., and Bayat, A. (2016). Evaluation of spring load restrictions and winter weight premium duration prediction methods in cold regions according to field data. *Canadian Journal of Civil Engineering, 43*(7), 667-674.

Attoh-Okine, N., and Adarkwa, O. (2013). Pavement Condition Surveys–Overview of Current Practices. *Delaware Center for Transportation, University of Delaware: Newark, DE, USA*.

Manik, B., and Pandey, B. (2008). Back Calculation of Layer Moduli of Concrete Pavement by Falling Weight Deflectometer, December 2008

Bennett, C. (1996). Calibrating road roughness meters in developing countries. *Transportation Research Record: Journal of the Transportation Research Board*(1536), 73-81.

C-SHRP, Canadian strategic Highway Research Program. (2000). Seasonal Load Restriction in Canada and Around the World 8.

Canada, Statistics. (2017). weather conditions in capital and major cities. Retrieved from http://www.statcan.gc.ca/tables-tableaux/sum-som/l01/cst01/phys08a-eng.htm

Crowder, J., and Shalapy, A. (2008). Assessing Spring Load Restrictions Using Climate Change and Mechanistic-EmpRIcal Distress Models.

Doré, G., Drouin, P., Pierre, P., and Desrochers, P. (2005). Estimation of the relationships of road deterioration to traffic and weather in Canada. *Transport Canada, Final Report*.

Doré, G., and Zubeck, K. (2009). *Cold regions pavement engineering 2009*.

Douangphachanh, V., and Oneyama, H. (2013). A study on the use of smartphones for road roughness condition estimation. *Journal of the Eastern Asia Society for Transportation Studies, 10*, 1551-1564.

Eagleson, B., Heisey, S., Hudson, W., Ronald, M., Alvin, H., and Stokoe, K. (1982). *Comparison of the falling weight deflectometer and the dynaflect for pavement evaluation*. Retrieved from

Government, Canada. (2017). Environmental and Natural Resources, Wether Climate and Hazards, Historical Data. Retrieved from http://climate.weather.gc.ca/climate_data/daily_data_e.html?StationID=51157&timeframe=2&StartYear=1840&EndYear=2017&Day=12&Year=2016&Month=5#

Haas, R., Li, N., and Tighe, S. (1999). *Roughness trends at C-SHRP LTPP sites*.

Hanson, T., Cameron, C., and Hildebrand, E. (2014). Evaluation of low-cost consumer-level mobile phone technology for measuring international roughness index (RI) values. *Canadian Journal of Civil Engineering, 41*(9), 819-827.

Hu, F. (2004). *Development of a direct type road roughness evaluation system.* University of South Florida.

Katicha, S., El Khoury, J., and Flintsch, G. (2016). Assessing the effectiveness of probe vehicle acceleration measurements in estimating road roughness. *International Journal of Pavement Engineering, 17*(8), 698-708.

Levinson, D., Marasteanu, M., Voller, V., Margineau, I., Smalkowski, B., Hashami, M., and Lukanen, E. (2005). Cost/Benefit Study of Spring Load Restrictions.

Mactutis, J., Alavi, S., and Ott, W. (2000). Investigation of relationship between roughness and pavement surface distress based on WesTrack project. *Transportation Research Record: Journal of the Transportation Research Board*(1699), 107-113.

Mahoney, J., Rutherford, M., and Hicks, R. (1987). *Guidelines for spring highway use restrictions*. Retrieved from

Ministère des Transports, de la Mobilité durable et de l'Électrification des transports. (2017a). Retrieved from www.transports.gouv.qc.ca

Ministère des Transports, de la Mobilité durable et de l'Électrification des transports. (2017b). *Thaw Report, Protecting the Road Network Is A Priority*. Retrieved from https://www.transports.gouv.qc.ca/en/trucking/Documents/fiches_degel_ang.pdf

Ministère des Transports, de la Mobilité durable et de l'Électrification des transports. (2017c). Thaw Zones. Retrieved from https://www.transports.gouv.qc.ca/en/trucking/Pages/zones-degel.aspx

Múčka, P. (2017). International Roughness Index specifications around the world. *Road Materials and Pavement Design, 18*(4), 929-965.

Ovik, J., Siekmeier, J., and Van Deusen, D. (2000). Improved Spring Load Restriction Guidelines Using Mechanistic Analysis.

Salour, F. (2015). *Moisture Influence on Structural Behaviour of Pavements: Field and Laboratory Investigations.* KTH Royal Institute of Technology.

Salour, F., & Erlingsson, S. (2012). Pavement structural behaviour during spring thaw: interpretation of FWD measurements by monitoring environmental data from county road 126 at Torpsbruk.

Sayers, M. (1995). On the calculation of international roughness index from longitudinal road profile. *Transportation Research Record* (1501).

Sayers, M., and Karamihas, S. (1998). The little book of profiling. *the Regent of the University of Michigan, 2*.

Schaus, L., and Popik, M. (2011). *Frost Heaves: A Problem That Continues To Swell*.

Shah, Y., Jain, S., Tiwari, D., and Jain, MK. (2013). Development of overall pavement condition index for urban road network. *Procedia-Social and Behavioral Sciences, 104*, 332-341.

Smith, T., Tighe, S., and Fung, R. (2001). *Concrete pavements in Canada: A review of their usage and performance.* Paper presented at the The Pavement Technology Advancements Session of the 2001 Annual Conference of the Transportation Association of Canada. Halifax, Nova Scotia.

Steinert, C., Humphrey, N., and Kestler, A. (2005). *Portable falling weight deflectometer study*. Retrieved from

TAC, Transportation Association of Canada. (2014). Pavement Asset Design and Managemnt

Talvik, O., and Aavik, A. (2009). Use of FWD deflection basin parameters (SCI, BDI, BCI) for pavement condition assessment. *The Baltic Journal of Road and Bridge Engineering, 4*(4), 196-196.

CNC, MTO and ARA. (2015). Infrastructure optimizing road infrastructure investments and accountability. Canadian National Committee (CNC) of the World Road Association in Partnership with Ontario Ministry of Transportation (MTO) and Applied Research Associates (ARA. *XXVth World Road Congress Seoul 2015).*

Yi, J., Doré, G., and Bilodeau, J.P. (2016). Monitoring and Modeling the Variations of Structural Behavior of a Flexible Pavement Structure during Freezing. *Journal of Cold Regions Engineering, 30*(4), 04016004.

Appendix

Date/Time	Year	Month	Day	Data Quality	Max Temp (°C)	Min Temp (°C)
24-09-16	2016	9	24	‡	17.7	5.6
25-09-16	2016	9	25	‡	17.1	6.1
26-09-16	2016	9	26	‡	18.3	4.3
27-09-16	2016	9	27	‡	20.9	11.9
28-09-16	2016	9	28	‡	21	10.1
29-09-16	2016	9	29	‡	18.2	8.1
30-09-16	2016	9	30	‡	18.8	8
01-10-16	2016	10	1	‡	18.1	11.6
02-10-16	2016	10	2	‡	16	13.1
03-10-16	2016	10	3	‡	19.4	8.5
04-10-16	2016	10	4	‡	19.3	5.1
05-10-16	2016	10	5	‡	20.5	7.6
06-10-16	2016	10	6	‡	23.4	8.8
07-10-16	2016	10	7	‡	25	9.9
08-10-16	2016	10	8	‡	17.6	10.6
09-10-16	2016	10	9	‡	13.8	4.8
10-10-16	2016	10	10	‡	11.8	2.6
11-10-16	2016	10	11	‡	16.7	3.1
12-10-16	2016	10	12	‡	20.2	8.8
13-10-16	2016	10	13	‡	14.4	3.7
14-10-16	2016	10	14	‡	10.7	0.7
15-10-16	2016	10	15	‡	16	4.5
16-10-16	2016	10	16	‡	18.3	11.3
17-10-16	2016	10	17	‡	15.6	8.2
18-10-16	2016	10	18	‡	24.3	8.4
19-10-16	2016	10	19	‡	17.1	9.1
20-10-16	2016	10	20	‡	12.4	7.5
21-10-16	2016	10	21	‡	10.3	7.8
22-10-16	2016	10	22	‡	8.1	2.6

Date/Time	Year	Month	Day	Data Quality	Max Temp (°C)	Min Temp (°C)
23-10-16	2016	10	23	‡	10.2	3.2
24-10-16	2016	10	24	‡	7	3
25-10-16	2016	10	25	‡	6.9	-0.6
26-10-16	2016	10	26	‡	3.4	-0.8
27-10-16	2016	10	27	‡	6.2	-1
28-10-16	2016	10	28	‡	5.7	3.7
29-10-16	2016	10	29	‡	7.7	3.2
30-10-16	2016	10	30	‡	6.5	4.1
31-10-16	2016	10	31	‡	4.6	1.6
01-11-16	2016	11	1	‡	11.2	-0.3
02-11-16	2016	11	2	‡	15.2	6.6
03-11-16	2016	11	3	‡	10.7	5.6
04-11-16	2016	11	4	‡	5.6	0.5
05-11-16	2016	11	5	‡	8.6	2.2
06-11-16	2016	11	6	‡	9.1	-1.6
07-11-16	2016	11	7	‡	10.8	-3
08-11-16	2016	11	8	‡	16	0.8
09-11-16	2016	11	9	‡	10	-0.8
10-11-16	2016	11	10	‡	12.3	-1.9
11-11-16	2016	11	11	‡	11.8	-1.3
12-11-16	2016	11	12	‡	7.4	-3.3
13-11-16	2016	11	13	‡	11	6.3
14-11-16	2016	11	14	‡	13.1	4.7
15-11-16	2016	11	15	‡	11.8	2.3
16-11-16	2016	11	16	‡	7.9	5.7
17-11-16	2016	11	17	‡	10.4	1.6
18-11-16	2016	11	18	‡	8.6	-1.1
19-11-16	2016	11	19	‡	9.6	2.3
20-11-16	2016	11	20	‡	6.2	-0.5
21-11-16	2016	11	21	‡	-0.5	-2.4
22-11-16	2016	11	22	‡	-0.1	-1.8
23-11-16	2016	11	23	‡	-0.1	-3.8
24-11-16	2016	11	24	‡	0.6	-1.6
25-11-16	2016	11	25	‡	1.4	0.1
26-11-16	2016	11	26	‡	2.5	-0.6
27-11-16	2016	11	27	‡	2.3	-0.4
28-11-16	2016	11	28	‡	-0.3	-2.8
29-11-16	2016	11	29	‡	2.2	-1.6
30-11-16	2016	11	30	‡	8.2	1.2
01-12-16	2016	12	1	‡	8.5	4.5
02-12-16	2016	12	2	‡	5.8	1.7

Date/Time	Year	Month	Day	Data Quality	Max Temp (°C)	Min Temp (°C)
03-12-16	2016	12	3	‡	3.5	-0.4
04-12-16	2016	12	4	‡	1.2	-3.9
05-12-16	2016	12	5	‡	-2.2	-5.5
06-12-16	2016	12	6	‡	1.3	-7
07-12-16	2016	12	7	‡	3.1	-1.7
08-12-16	2016	12	8	‡	2.3	-3.2
09-12-16	2016	12	9	‡	-3	-8.3
10-12-16	2016	12	10	‡	-5.2	-11.6
11-12-16	2016	12	11	‡	-3.8	-13.7
12-12-16	2016	12	12	‡	-2.6	-6.3
13-12-16	2016	12	13	‡	2.2	-7.5
14-12-16	2016	12	14	‡	-0.6	-8
15-12-16	2016	12	15	‡	-7.7	-20.5
16-12-16	2016	12	16	‡	-15.3	-23.5
17-12-16	2016	12	17	‡	-7.6	-15.7
18-12-16	2016	12	18	‡	-3.6	-17.3
19-12-16	2016	12	19	‡	-11.2	-22.5
20-12-16	2016	12	20	‡	-0.1	-17.1
21-12-16	2016	12	21	‡	2.3	-0.4
22-12-16	2016	12	22	‡	1.1	-0.4
23-12-16	2016	12	23	‡	1.9	-0.5
24-12-16	2016	12	24	‡	3	-0.4
25-12-16	2016	12	25	‡	2.9	-11.3
26-12-16	2016	12	26	‡	2.2	-12.6
27-12-16	2016	12	27	‡	7.1	-0.3
28-12-16	2016	12	28	‡	-0.2	-8.2
29-12-16	2016	12	29	‡	0.7	-6.6
30-12-16	2016	12	30	‡	-1.6	-11.4
31-12-16	2016	12	31	‡	-8.6	-15.3
01-01-17	2017	1	1	‡	-2.4	-8.7
02-01-17	2017	1	2	‡	1.8	-10.2
03-01-17	2017	1	3	‡	0.5	-5.8
04-01-17	2017	1	4	‡	2.5	-5.6
05-01-17	2017	1	5	‡	-5.3	-10.7
06-01-17	2017	1	6	‡	-7.7	-16.4
07-01-17	2017	1	7	‡	-9.6	-18.9
08-01-17	2017	1	8	‡	-10.9	-20.3
09-01-17	2017	1	9	‡	-7	-21.9
10-01-17	2017	1	10	‡	1.3	-8.3
11-01-17	2017	1	11	‡	5.7	1.2

Date/Time	Year	Month	Day	Data Quality	Max Temp (°C)	Min Temp (°C)
12-01-17	2017	1	12	‡	5	-0.9
13-01-17	2017	1	13	‡	-0.4	-14.9
14-01-17	2017	1	14	‡	-7.1	-17.2
15-01-17	2017	1	15	‡	-7.4	-11.3
16-01-17	2017	1	16	‡	2.7	-9
17-01-17	2017	1	17	‡	-0.4	-5.3
18-01-17	2017	1	18	‡	-1.3	-5.3
19-01-17	2017	1	19	‡	2	-1.3
20-01-17	2017	1	20	‡	2.2	0.2
21-01-17	2017	1	21	‡	2.1	0.3
22-01-17	2017	1	22	‡	2.1	-2.6
23-01-17	2017	1	23	‡	-0.1	-3.8
24-01-17	2017	1	24	‡	-2.3	-3.8
25-01-17	2017	1	25	‡	0.3	-2.4
26-01-17	2017	1	26	‡	1.4	0.1
27-01-17	2017	1	27	‡	0.8	-3.1
28-01-17	2017	1	28	‡	0.2	-3
29-01-17	2017	1	29	‡	-0.3	-6.5
30-01-17	2017	1	30	‡	-6.4	-13.7
31-01-17	2017	1	31	‡	-7.2	-17.6
01-02-17	2017	2	1	‡	-6.3	-13.9
02-02-17	2017	2	2	‡	-5.7	-10.7
03-02-17	2017	2	3	‡	-5.3	-9.9
04-02-17	2017	2	4	‡	-3.4	-13.2
05-02-17	2017	2	5	‡	-0.4	-7.7
06-02-17	2017	2	6	‡	-7.6	-13.6
07-02-17	2017	2	7	‡	1.1	-12
08-02-17	2017	2	8	‡	3.9	-9.8
09-02-17	2017	2	9	‡	-9.8	-15.3
10-02-17	2017	2	10	‡	-12.9	-16.2
11-02-17	2017	2	11	‡	-10.4	-13.9
12-02-17	2017	2	12	‡	-2.9	-13.6
13-02-17	2017	2	13	‡	-3	-8
14-02-17	2017	2	14	‡	-3.5	-11.9
15-02-17	2017	2	15	‡	-2.8	-6.4
16-02-17	2017	2	16	‡	-2	-4.9
17-02-17	2017	2	17	‡	-2.8	-9.1
18-02-17	2017	2	18	‡	7.6	-5.7
19-02-17	2017	2	19	‡	8	0.5
20-02-17	2017	2	20	‡	0.5	-7
21-02-17	2017	2	21	‡	3.3	-8.2

Date/Time	Year	Month	Day	Data Quality	Max Temp (°C)	Min Temp (°C)
22-02-17	2017	2	22	‡	6.5	0
23-02-17	2017	2	23	‡	12.3	1.4
24-02-17	2017	2	24	‡	4.4	0.6
25-02-17	2017	2	25	‡	14.5	0.1
26-02-17	2017	2	26	‡	1.9	-4.8
27-02-17	2017	2	27	‡	5.6	-2
28-02-17	2017	2	28	‡	8.3	-4.6
01-03-17	2017	3	1	‡	7.3	1.9
02-03-17	2017	3	2	‡	5.5	-10.2
03-03-17	2017	3	3	‡	-8	-14.3
04-03-17	2017	3	4	‡	-12.3	-17.6
05-03-17	2017	3	5	‡	-6.2	-17.5
06-03-17	2017	3	6	‡	0.7	-12.9
07-03-17	2017	3	7	‡	6	-2.9
08-03-17	2017	3	8	‡	10.4	1.2
09-03-17	2017	3	9	‡	1.9	-5.9
10-03-17	2017	3	10	‡	-4.8	-19
11-03-17	2017	3	11	‡	-15.2	-20.8
12-03-17	2017	3	12	‡	-10.3	-17.2
13-03-17	2017	3	13	‡	-8.3	-15.8
14-03-17	2017	3	14	‡	-7.6	-9.3
15-03-17	2017	3	15	‡	-4.2	-8.1
16-03-17	2017	3	16	‡	-3.4	-9.9
17-03-17	2017	3	17	‡	-2.3	-12
18-03-17	2017	3	18	‡	0.4	-15
19-03-17	2017	3	19	‡	3	-9.2
20-03-17	2017	3	20	‡	5.1	-7.5
21-03-17	2017	3	21	‡	3.6	-3
22-03-17	2017	3	22	‡	-3.1	-13.2
23-03-17	2017	3	23	‡	0.3	-11.4
24-03-17	2017	3	24	‡	0.1	-2.7
25-03-17	2017	3	25	‡	2.3	-7.9
26-03-17	2017	3	26	‡	1.5	-8.1
27-03-17	2017	3	27	‡	4	1
28-03-17	2017	3	28	‡	4.8	0.8
29-03-17	2017	3	29	‡	6.3	1.7
30-03-17	2017	3	30	‡	5.6	-0.3
31-03-17	2017	3	31	‡	5.2	0.1
01-04-17	2017	4	1	‡	2.4	0.2
02-04-17	2017	4	2	‡	9.9	-0.6
03-04-17	2017	4	3	‡	8.7	-2.4

Date/Time	Year	Month	Day	Data Quality	Max Temp (°C)	Min Temp (°C)
04-04-17	2017	4	4	‡	5.6	2.1
05-04-17	2017	4	5	‡	7.6	3.8
06-04-17	2017	4	6	‡	5.1	2
07-04-17	2017	4	7	‡	5.5	1.4
08-04-17	2017	4	8	‡	8.2	0.4
09-04-17	2017	4	9	‡	16	-2.2
10-04-17	2017	4	10	‡	25.6	8.2
11-04-17	2017	4	11	‡	14.1	4.7
12-04-17	2017	4	12	‡	10.1	4.2
13-04-17	2017	4	13	‡	14.2	1.8
14-04-17	2017	4	14	‡	14.3	-0.8
15-04-17	2017	4	15	‡	19	2.9
16-04-17	2017	4	16	‡	15.6	8
17-04-17	2017	4	17	‡	8.8	3.4
18-04-17	2017	4	18	‡	9.5	0.6
19-04-17	2017	4	19	‡	9.7	5.3
20-04-17	2017	4	20	‡	10	5.2
21-04-17	2017	4	21	‡	12.2	6.9
22-04-17	2017	4	22	‡	9.7	4.1
23-04-17	2017	4	23	‡	18	0.7
24-04-17	2017	4	24	‡	9.5	0.4
25-04-17	2017	4	25	‡	15.2	1.8
26-04-17	2017	4	26	‡	16.2	8.8
27-04-17	2017	4	27	‡	25.3	10.3
28-04-17	2017	4	28	‡	20.8	9.4
29-04-17	2017	4	29	‡	19.4	4.4
30-04-17	2017	4	30	‡	7.1	1.7
01-05-17	2017	5	1	‡	9.7	5.5
02-05-17	2017	5	2	‡	16.4	7.5
03-05-17	2017	5	3	‡	12.8	3.1
04-05-17	2017	5	4	‡	16.2	2.2
05-05-17	2017	5	5	‡	10	6.8
06-05-17	2017	5	6	‡	21.9	6.8
07-05-17	2017	5	7	‡	10.5	3.2
08-05-17	2017	5	8	‡	6.1	0.8
09-05-17	2017	5	9	‡	8.8	0.6
10-05-17	2017	5	10	‡	12.6	2.5
11-05-17	2017	5	11	‡	13.2	6
12-05-17	2017	5	12	‡	18.7	7.1
13-05-17	2017	5	13	‡	18.9	9
14-05-17	2017	5	14	‡	13.1	8.8

Date/Time	Year	Month	Day	Data Quality	Max Temp (°C)	Min Temp (°C)
15-05-17	2017	5	15	‡	22.8	9.3
16-05-17	2017	5	16	‡	22.9	7.9
17-05-17	2017	5	17	‡	29.3	14.1
18-05-17	2017	5	18	‡	30.4	18.7
19-05-17	2017	5	19	‡	19.6	8
20-05-17	2017	5	20	‡	18.2	5.6